TITLE PAGE

Evaluating the effects of China's pollution controls on inter-annual trends and uncertainties of atmospheric mercury emissions

Yu Zhao[1, 2*], Hui Zhong[1], Jie Zhang[2, 3], Chris P. Nielsen[4]

1. State Key Laboratory of Pollution Control & Resource Reuse and School of the Environment, Nanjing University, 163 Xianlin Ave., Nanjing, Jiangsu 210023, China

2. Collaborative Innovation Center of Atmospheric Environment and Equipment Technology, CICAEET, Nanjing, Jiangsu 210044, China

3. Jiangsu Provincial Academy of Environmental Science, 176 North Jiangdong Rd., Nanjing, Jiangsu 210036, China

4. Harvard China Project, School of Engineering and Applied Sciences, Harvard University, 29 Oxford St, Cambridge, MA 02138, USA

*Corresponding author: Yu Zhao

Phone: 86-25-89680650; email: yuzhao@nju.edu.cn

ABSTRACT

China's anthropogenic emissions of atmospheric mercury (Hg) have been effectively constrained by national air pollution control and energy efficiency policies. Improved methods, based on available field measurements, are developed to quantify the benefits of Hg abatement by various emission control measures. Those measures include increased use of (1) flue gas desulfurization (FGD) and selective catalyst reduction (SCR) systems in power generation; (2) precalciner kilns with fabric filters (FF) in cement production; (3) mechanized coking ovens with electrostatic precipitators (ESP) in iron & steel production; and (4) advanced production technologies in nonferrous metal smelting. Investigation reveals declining trends in emission factors for each of these sources, which together drive a much slower growth of total Hg emissions than the growth of China's energy consumption and economy, from 679 metric tons (t) in 2005 to 750 t in 2012. In particular, estimated emissions from the above-mentioned four source types declined nearly 50% from 2005 to 2012, which can be attributed to expanded deployment of technologies with higher energy efficiencies and air pollutant removal rates. The species shares of total Hg emissions have been stable in recent years, with mass fractions of around 55%, 39%, and 6% for Hg^0, Hg^{2+}, and Hg^p, respectively. The higher estimate of total Hg emissions than previous inventories is supported by limited simulation of atmospheric chemistry and transport, but middle- to long-term observations of ambient Hg levels are needed to verify the inter-annual emission trends. With improved implementation of emission controls and energy saving, a 23% reduction in annual Hg emissions from 2012 to 2030, to below 600 t, is expected in the most optimistic of several scenarios. While growth in Hg emissions has been gradually constrained, uncertainties quantified by Monte-Carlo simulation for recent years have increased, particularly for the power sector and particular industrial sources. The uncertainty

41 (expressed as 95% confidence intervals) of Hg emissions from coal-fired power plants, for example,
42 increased from -48%–+73% in 2005 to -50%–+89% in 2012. This is attributed mainly to swiftly
43 increased penetration of advanced manufacturing and pollutant control technologies; the unclear
44 operational status and relatively small sample sizes of field measurements of those processes have
45 resulted in lower but highly varied emission factors. To reduce uncertainty and further confirm the
46 benefits of pollution control and energy polices, therefore, systematic investigation of specific Hg
47 pollution sources is recommended. The variability of temporal trends and spatial distributions of Hg
48 emissions need to be better tracked during the ongoing dramatic changes in China's economy, energy
49 use, and air pollution status.
50

51 **1 INTRODUCTION**

52 Increasing international efforts have been made to study and control mercury (Hg), a pollutant
53 well-known for its toxicity and long-range transport. Atmospheric emissions are identified as the most
54 significant pathway of Hg release into the environment (Pirrone and Mason, 2009). In contrast to
55 other heavy metals that are mainly associated with air particles, atmospheric Hg includes several
56 forms: gaseous elemental Hg (GEM, Hg^0), which has the longest atmospheric lifetime and transport
57 distance; reactive gaseous mercury (RGM, Hg^{2+}), which is generally derived from more local sources;
58 and particle-bound mercury (PBM, Hg^p).
59 Available global emission inventories indicate that China has become the highest ranking nation
60 in anthropogenic Hg emissions, attributed mainly to intensive use of fossil fuels to serve a large and
61 rapidly growing economy (Fu et al., 2012a; Pacyna et al., 2010; Pirrone et al., 2010). Pacyna et al.
62 (2010) calculated China's Hg emissions from fossil fuel use at 400 metric tons (t) in 2005, almost half

of the country's anthropogenic emissions. Domestic field measurements or investigations of Hg emissions have also been conducted for other sources including cement production (Li, 2011), metals mining and smelting (P Li et al., 2009; Li et al., 2012; Li et al., 2010; Wang et al., 2010a; Wu et al., 2012), solid waste incineration (L Chen et al., 2013; Hu et al., 2012) and biomass burning (C Chen et al., 2013; Huang et al., 2011). Most current inventories, however, ignore differences in application of technologies and in country- or region-dependent parameters related to emissions, instead applying global emission factors to most sectors. As stressed by AMAP/UNEP (2013), research on the industrial processes and technologies employed to reduce Hg emissions in different industries, and more importantly in specific countries, is a priority to improve estimation of Hg emissions.

Under strong pressure to improve air quality (and to strengthen energy security and limit carbon), China's government has been implementing a series of measures to conserve energy and control emissions. Since 2005, for example, small and inefficient plants or boilers in the power sector and certain heavy industrial sectors including cement and steel production have been gradually replaced with larger, energy-efficient ones that include advanced dust collectors. Installation of flue gas desulfurization (FGD) systems have been compulsory at all new thermal power units to abate SO_2 emissions, and the FGD penetration has increased from 13% of total thermal power capacity in 2005 to 86% in 2010 (Zhao et al., 2008; 2013). Since 2010, selective catalyst reduction (SCR) systems have been increasingly installed in power plants to reduce NO_X emissions, and the penetration is expected to rise from 10% in 2010 to 70% in 2015 (Wang, 2013). The 2013 announcement of a national action plan of air pollution control, responding to recent severe urban haze episodes, will result in further advances in emission abatement and air quality in the future (Zhao et al., 2014). Although designed to target other pollutants, all of these measures have ancillary benefits to atmospheric Hg abatement. For example, the use of advanced dust collectors (e.g., fabric filters (FF) and electrostatic precipitators

86 (ESP)) and FGD are expected to significantly reduce emission levels by capturing some Hg in fly ash
87 and gypsum byproduct (USEPA, 2002a; Wang et al., 2010b). SCR catalysts convert part of the Hg^0 to
88 Hg^{2+}, which is more liable to be absorbed by the FGD scrubber (Wang et al., 2012; Tian et al., 2012).
89 Failure to track and evaluate such swift changes in emission sources and control technologies will
90 lead to less accurate estimates of the trends in China's Hg emissions and its contributions to the global
91 Hg cycle. Currently, most global estimates of historical and future Hg emissions show steadily
92 increasing trends, driven mainly by expansion of industry in Asia (Streets et al., 2009a; Driscoll et al.,
93 2013; AMAP/UNEP, 2013). This is inconsistent, however, with declining worldwide trends in
94 background atmospheric Hg concentrations (Slemr et al., 2011; Ci et al., 2012; Driscoll et al., 2013).
95 Aside from the implications of recent and future trends, the Hg emission uncertainties pose
96 further problems to the scientific community. The uncertainties will be transferred by use of the
97 emission estimates in atmospheric chemistry simulations to analyses of transport and deposition of Hg
98 (Pan et al., 2008; Lin et al., 2010; Corbitt et al., 2011). Despite this, very few countries include
99 quantified uncertainties in their national emission reporting, particularly developing countries with
100 poorer data availability and quality including China (Pacyna et al., 2010; Ci et al., 2012;
101 AMAP/UNEP, 2013). To date, only the uncertainties of emissions from the power sector have been
102 systematically quantified for China (Wu et al., 2010), with the lack of estimates for other sectors
103 attributed mainly to limited information about other emission source types.
104 This study therefore seeks to assess the effects of recently implemented and ongoing control
105 measures on past and future inter-annual trends and sector distributions of China's anthropogenic Hg
106 emissions. The uncertainty of emissions is quantified, and the most sensitive parameters identified for
107 improvement of future estimates. Section 2 briefly describes the methodology of emission inventory
108 development, stressing improved data and methods for particular emission sources, the basic

assumptions underlying future emission scenarios, and the Monte-Carlo framework of uncertainty analysis. Section 3 is a thorough analysis of Hg emission factors by species, sector, and year, incorporating the latest information about emission control strategies and data from domestic field measurements and investigations. Section 4 presents China's recent (2005-2012) trends in anthropogenic Hg emissions and future (to 2030) trajectories by scenario, evaluation of the effects of pollution control measures, comparison of emission estimates with those of other studies, and the uncertainties of estimates, including the main sources of uncertainty. Section 5 summarizes the study.

2 METHODOLOGY AND DATA SOURCES

2.1 Brief summary of Hg emission estimation

The research domain covers the 31 provinces of mainland China. Annual emissions of Hg, including speciated forms (Hg^0, Hg^{2+}, and Hg^p), are estimated at the provincial level from 2005 to 2012, to evaluate the effects of China's energy policies and air pollution control measures. The main anthropogenic activities fall into three sector categories: coal-fired power plants (CPP), all other industrial facilities (IND), and the residential & commercial sector (RES). IND is further divided into cement kilns (CEM), iron & steel plants (ISP), heating boilers (HB), other industrial boilers (OIB), nonferrous metal smelting plants (NMS), gold mining operations (GM, including large-scale gold mining, LGM, and artisanal and small-scale gold mining, ASGM), and the operations of other miscellaneous processes (OMP). RES mainly includes coal combustion (RC), oil & gas combustion (ROG), biofuel use/biomass open burning (BIO), and solid waste incineration (SWI) subcategories. As the dominant primary energy resource, coal plays important roles in most anthropogenic pollutant emissions in China (Zhao et al., 2013). In this work, therefore, the Hg emissions from coal use are

estimated based on the above-mentioned source categories, e.g., power plants, industrial boilers, residential coal stoves, and iron & steel production (most emissions of which come from coal use). For cement production, Hg emissions result both from coal combustion and non-combustion processes, and a new method is developed to differentiate the two parts, as described in Section 2.2.

In general, annual emissions of total Hg and the three Hg species are calculated using Eq. (1) and (2), respectively, for a given province *i* and a given year *t*:

$$E_{i,t} = \sum_{m}\sum_{n} AL_{m,n,i,t} \times EF_{m,n,i,t} \quad (1)$$

$$E_{i,t,s} = \sum_{m}\sum_{n} AL_{m,n,i,t} \times EF_{m,n,i,t} \times f_{m,n} \quad (2)$$

where E is the Hg emission; AL is the activity levels (fuel consumption or industrial production), EF is the combined emission factor (emissions per unit of activity level); f is the mass fraction of a given Hg species (Hg^0, Hg^{2+} or Hg^p); and i, t, m, n and s represent province, year, emission source type, technology of manufacturing and emission control, and Hg species.

For coal combustion, Eq. (1) can be further revised to Eq. (3) with detailed combustor and fuel information:

$$E_{i,t} = \sum_{m}\sum_{n} AL_{m,n,i,t} \times HgC_{i,t} \times R_{m,n} \times \left(1 - \eta_{m,n,t}\right) \quad (3)$$

where HgC is the Hg content of coal by province; R is the mass fraction of Hg released from the fuel; and η is Hg removal efficiency of air pollution control devices.

Due to inadequate information, emissions from ASGM are not calculated based on the emission factors and activity levels in this work. ASGM was officially prohibited in the 1990s, although it may still occur illegally in some areas because of the huge economic profits. Telmer and Veiga (2009) estimated the Hg release from ASGM in 2008 based on available data on Hg and gold exports and imports, and the results are widely accepted (AMAP/UNEP, 2013). Muntean et al. (2014) developed a

153 new method to estimate historical trends in ASGM activity, based on the market demand for gold and
154 the relatively accurate data available on large-scale gold production. They found little inter-annual
155 variation after 2005 for China. In this work, therefore, the results by Telmer and Veiga (2009) are
156 directly used for 2005-2012.

157 Activity levels for 2005-2012 are compiled annually by sector from various data sources.
158 Multiple-year fossil fuel consumption and industrial production at the provincial level are obtained
159 from Chinese official energy (NBS, 2013a) and industrial economic statistics (NBS, 2013b),
160 respectively. The coal consumption in CEM and ISP is calculated following the methods of Zhao et al.
161 (2011; 2012), and the coal consumption by OIB is estimated by subtracting the fuel consumed by
162 CEM, ISP, and HB from that by IND (Zhao et al., 2012). The annual biofuel use until 2008 is taken
163 from official statistics (NBS, 2013a); NBS stopped reporting the data in that year, so estimates for
164 subsequent years are taken from unpublished data of the Ministry of Agriculture (C Chen et al., 2013).
165 The biomass combusted in open fields is calculated as a product of grain production, waste-to-grain
166 ratio, and the percentage of residual material burned in the field, as described in Zhao et al. (2011;
167 2012). The burned urban municipal waste is taken from official statistics (NBS, 2013c), and that in
168 rural areas is calculated as a product of rural population, the average waste per capita, and the
169 estimated ratios of waste that is burned (Yao et al., 2009).

170 The Hg emission factors, speciation, and the time-series trends due to improved controls will be
171 described by sector in Section 3.

172 **2.2 Improved methods for estimating emissions from particular sources**

173 Emission estimation methods for certain sources are improved in this work to better understand
174 the effectiveness of ongoing pollution control measures in China. Those sources include thermal
175 power generation, cement and steel production, and nonferrous metal smelting, emissions of which

were estimated in previous studies with uniform, time-independent emission factors averaged at the sector level.

For power plants, detailed information related to emission estimation are compiled at the generating unit-level, including coal consumption, combustion technology, fuel quality, and the time and type of emission control technologies applied, based on an updated Chinese power plant database developed by the authors (Zhao et al., 2008). Hg emissions of each plant are then calculated plant-by-plant based on the unit-specific information using Eq. (3).

With improved data on kiln technologies and emission control devices (Lei et al., 2011; Zhao et al., 2013), their penetrations into the cement industry for a range of years are derived in this work. Hg emission factors by emission control type, based on domestic measurements, are accordingly applied to generate the inter-annual trends in emissions. Besides total emissions of the sector, Equation (3) is used to separately estimate the emissions from coal combustion in cement industry. For nonferrous metal smelting, similarly, the penetrations of different manufacturing technologies for typical years (2005, 2007, and 2010) are obtained from a plant-by-plant database developed by Tsinghua University (Wu et al., 2012), and penetrations for other years have to be interpolated due to lack of further information. The inter-annual trends of emissions can then be estimated by combining the penetration and emission factors by technology.

For iron & steel production, Hg emissions come mainly from coal-combustion processes including coking, sintering, and pig-iron production. In recent years, implementation of national energy-saving and pollution-control policies led to improved energy efficiency and enhanced use of emission control devices of those processes (Zhao et al., 2013). The updated information is integrated into Eq. (3) to estimate the Hg emissions for the sector by process and year. In particular, the coal

consumption by process is calculated based on the amount of coal combusted by the whole sector and the energy efficiency by process (expressed as kg coal-equivalent/t-steel) reported in official statistics.

2.3 Uncertainty analysis

The uncertainties of Hg emissions, including by different species, are quantified by sector and year using a Monte-Carlo framework developed by Zhao et al. (2011). Probability distributions are estimated for all input parameters, and 10,000 simulations are then performed to estimate the uncertainties of emissions and to identify the crucial parameters that significantly contribute to the uncertainties for different source types.

In most cases, the uncertainties of activity levels (including penetration rates of different technologies by sector) are determined following our previous work (Zhao et al., 2011; 2013). Generally, normal distributions are assumed for fuel consumption and industrial and agricultural production, with coefficients of variation (CV, the standard deviation divided by the mean) set at 5%, 10%, and 20% for power, industry, and residential & commercial sectors, respectively. A comprehensive analysis of uncertainties of Hg emission factors was conducted by sector and species, with domestic field measurements thoroughly evaluated. For parameters with adequate measurement data, the Kolmogorov-Smirnov test for the goodness-of-fit ($p=0.05$) is applied and, if the test is passed, bootstrap simulation is conducted to determine the probability distribution (Frey and Zheng, 2002; Zhao et al., 2010; 2011). For parameters that fail to pass the goodness-of-fit test or those with limited observational data, probability distributions must be assumed based on previous work (e.g., Wu et al., 2010) and/or the authors' judgments. Details about the emission factor uncertainties by sector will be discussed in Section 3.

For ASGM, in which emissions were not calculated but taken directly from Telmer and Veiga (2009) as described in section 2.2, the uncertainties are assumed at ±67% according to expert judgment (AMAP/UNEP, 2013). Muntean et al. (2014) compared the ASGM emissions estimated from varied methods and data sources (AGC, 2010; Telmer and Veiga, 2009), and the differences are within the uncertainty range assumed in this work.

2.4 Emission projections to 2030

Three scenarios are devised to project China's atmospheric Hg emissions in 2015, 2020, and 2030. Scenario 0 (S0) is the most conservative case, in which the national policy of energy saving and air pollution control will not change in practice after 2012. This does not imply, however, that the penetration levels of advanced technologies and emission control devices in specific sectors will necessarily be the same as in 2012. For example, current policies for the power sector will undoubtedly raise the use of FGD and SCR systems, and that for cement will increase the share of precalciner kilns with FF systems (i.e., this share would reach 100% in 2030, compared to 88% in 2012). While keeping the control strategy the same as in S0, Scenario 1 (S1) integrates the national energy policy commitments that have been announced (e.g., the plans to reduce fossil energy use and to reduce greenhouse gas emissions) and thus illustrates the benefits of enhanced energy saving on Hg emissions. The activity-level data for S0 and S1 are taken respectively from the Current Policy Scenario (CPS) and New Policy Scenario (NPS) of our previous work (Zhao et al., 2014), which are based mainly on projections by IEA (2012), with revisions in specific sectors including power and transportation. For sources that are not mentioned in Zhao et al. (2014), specific working reports are consulted. For example, the burned ratio of urban municipal solid waste is assumed to reach 50% in 2030, according to CAUES (2013). Scenario 2 (S2) shares the same activity level trends as S1 but includes more stringent emission controls, mainly for industrial sources. Those measures include use

of advanced control devices specifically for Hg removal in new power plants, use of FGD systems in new industrial and heating boilers, use of SCR in new cement precalciner kilns starting in 2020, greater penetration of electric furnaces in steel smelting (resulting in less pig-iron production and thereby less coal combustion), and greater penetration of advanced manufacturing technologies, with lower Hg emission factors, in nonferrous metal smelting. The detailed control benefits of those technologies on Hg emissions are described in the next section.

3 EVOLUTION OF EMISSION FACTORS

3.1 Evolution of emission factors for key sectors, including key assumptions and uncertainties

The improvement of emission factors in this study result mainly from two sources: (1) new and better data that domestic measurements have made available for key sectors; and (2) better understanding of penetration levels of manufacturing and control technologies for different sources during 2005-2012. Those improvements provide more accurate emission factors, with clearer inter-annual trends by sector, as shown in Figure 1. Through comprehensive review of the literature, a database for Hg emission factors (and related parameters) by sector is established for China, with the uncertainty for each emission factor or parameter analyzed and presented as a probability distribution function (PDF), as summarized in Table 1.

Power plants

As Eq. (3) indicates, the integrated Hg emission factor for power plants, expressed in metric tons (t) of Hg emissions per million metric tons (Mt) coal combusted, is calculated as the product of the Hg content of coal, the release rate of the specific combustion facility, and the difference of one and the Hg removal efficiency of a specific air pollution control device (APCD).

The Hg content of coal in China has been addressed in a series of studies (Wang et al., 2000; Huang and Yang, 2002; Feng et al., 2002; USGS, 2004; Zheng et al., 2006; Zhang et al., 2012a), and the method of Wu et al. (2010) is followed in this work to determine the values and uncertainties by province. The percentages of Hg content by province are estimated based on available measurement data and a conservative assumption of a lognormal distribution is applied as the PDF, with relatively long tails for the distributions in most provinces. Regarding the release rates, the values for pulverized combustion (PC), circulating fluidized bed (CFB), and grate boiler systems reach 98.7%, 98.4%, and 95.9%, respectively, reflecting that most Hg in coal is emitted into the flue gas due to the high combustion temperature (see details in Table S1 in the Supplement). As currently available measurements are insufficient for data fitting to determine the uncertainties, triangular distributions are assumed for the parameter, with the lowest and highest measurement values taken as the 10^{th} and 90^{th} percentile of each distribution, respectively.

As the foremost emission control measure taken in China since 2005, deployment of advanced APCDs in the coal-fired power sector has increased swiftly. The penetration levels of FGD and SCR systems, for example, reached 90% and 27%, respectively, in 2012. These technologies demonstrably result in lower Hg emission factors and thereby ancillary benefits in Hg removal (Wang et al., 2012). In this work, the removal efficiencies of major types of APCDs, including ESP, FF, joint ESP and FGD (ESP+FGD), and joint SCR, ESP, and FGD (SCR+ESP+FGD), are analyzed using the most recent field measurements at China's power plants (see details in Table S2 in the Supplement). As shown in Figure 2, SCR+ESP+FGD systems have the highest Hg removal efficiency, at 76.6%, followed by FF at 56.1% and ESP+FGD at 53.8%. Large variations of Hg removal efficiencies of APCDs are indicated by different studies, and the values estimated and applied in this work are relatively conservative, particularly for ESP+FGD, which is currently the dominant APCD

configuration in China's power sector. In addition, the removal efficiencies are much lower than those in developed countries like the U.S. and Japan. Two reasons could be a large difference in coal qualities between the countries and the poorer operational conditions of APCDs in China (Li, 2011; Zhi et al., 2013). For other dust collectors including wet scrubbers (WET) and cyclones (CYC), limited domestic information from field tests can be obtained and used in this work (e.g., Huang et al., 2004), leading to higher removal efficiencies than previous inventories (Streets et al., 2005; Wu et al., 2006). We believe these values do not significantly raise the uncertainty because the capacity share of units with either WET or CYC is small, i.e., roughly 2% in 2010.

Regarding the prospects for further improvement of Hg emission control in the future, newly-built power units are assumed to apply powdered activated carbon (PAC) injection technology (Srivastava et al., 2006; Cui et al., 2011) or modified catalytic oxidation of elemental Hg (Guo et al., 2011; Yan et al., 2011) in S2, and the average Hg removal efficiencies of those technologies are expected to reach 90%. The PDFs of removal efficiencies by device are estimated following the description in Section 2.3. In most cases, the PDFs are assumed to be Weibull distributions due to insufficient data samples. For ESP, however, the data from currently available measurements pass the statistical test, and bootstrap simulation is thus conducted to determine a normal PDF, as shown in Figure S3(a) in the Supplement.

Due mainly to the sharply growing use of APCDs, the average Hg emission factor for power plants is estimated to have decreased from 0.13 g/t-coal in 2005 to 0.08 in 2012, as shown in Figure 1(a). With PAC injection applied in the future under S2, the average emission factor would further decline to 0.05 g/t-coal in 2030.

Iron & steel production

In previous studies, a uniform emission factor of 0.04 g/t-steel has generally been applied for iron & steel production, with little consideration of improving production technologies (Streets et al., 2005; Wu et al., 2006). In this work, as described in Section 2.2, the latest information on APCD penetration trends and removal efficiencies is combined, Hg emissions are calculated separately for each coal-consuming process using Eq. (3), and these are then aggregated to the sector level. The Hg release ratios of coking and pig-iron production are estimated at 63% and 84%, respectively (Wang et al., 2000; Hong et al., 2004), with uniform distributions conservatively assumed due to a lack of updated measurements. Without specific further information, the removal efficiencies and PDFs for the iron & steel industry are assumed to be the same as those for the power sector. This assumption is expected to result in a possible underestimate of emissions for the sector, because the APCD operations may not be as thorough as those at power plants, given the greater regulatory oversight of the latter in recent years. Although this possible underestimate could be partly quantified by uncertainty analysis, more investigation of the APCD benefits on Hg removal for the iron & steel sector is needed first (as is also the case with other non-power industrial sectors).

Driven by the increased penetration of advanced manufacturing and emission control technologies, in particular the growth of mechanized coking ovens, the emission factor for iron & steel production is estimated to have declined from 0.071 to 0.039 g/t-steel from 2005 to 2012, indicating that the application of 0.04 g/t-steel in earlier studies might have underestimated the emissions for this sector in previous years (Figure 1(b)). Regarding the future projection, the ratio of pig iron to steel is assumed to decrease from 92% in 2012 to 80% in 2030 in S2, due to expanding use of electric arc furnaces that use more waste-steel inputs instead of more energy-intensive inputs

330 including pig iron (Wang et al., 2007; Zhao et al., 2012). The emission factor would thus decline
331 further to 0.035 g/t-steel.

332 **Non-ferrous metal smelting**

333 Although the non-ferrous metal industry, including smelting of Pb, Zn, and Cu, is one of the
334 main sources of Hg emissions (Li et al., 2010; Wu et al., 2012), available emission factors from field
335 tests are still limited, given the many and complex factors that determine emission levels (e.g., the Hg
336 concentration in ore concentrate, smelting technology, and the penetration of acid plants and APCDs).
337 Based on these limited data, a process-based methodology is developed and applied in this work to
338 estimate the emission factors for various kinds of smelters employed in China, as shown in Table S3
339 in the Supplement. Information on all of the processes and their corresponding emission factors are
340 obtained from direct field measurements (Feng et al., 2004; G. Li et al., 2009; Li et al., 2010; Wang et
341 al., 2010; Zhang et al., 2012b) or field-based calculations (Wu et al. 2012). Given the very small
342 sample sizes, uniform distributions have to be assumed for most processes, with the lowest and
343 highest measurement values taken as the 10^{th} and 90^{th} percentile of each distribution, respectively.
344 Notably, the oxygen-pressure leaching process for Zinc smelting has not been included in the table,
345 because it does not include the process of high-temperature calcination and thus little mercury is
346 released to the atmosphere.

347 Based on a plant-by-plant database (Wu et al., 2012) and a list of small smelters that have been
348 shut down since 2010, the penetrations of various kinds of smelters are calculated by year and
349 non-ferrous metal type, and the inter-annual trends of emission factors are then analyzed. As shown in
350 Figure 1(d)-(f), the national average EFs for Zn, Pb, and Cu smelting are estimated to have dropped
351 from 15.5, 16.7, and 1.7 g/t-product in 2005 to 13.3, 4.7, and 0.2 g/t in 2012, respectively. In the
352 future projection of S2, the EFs are projected based on the assumption that the most advanced

353 technologies will be required at all new smelters. The EFs for Zn and Pb are thus estimated to decline
354 further to 9.1 and 2.2 g/t-product in 2030, respectively.

355 **Cement production**

356 A series of studies have been conducted to measure the Hg emission levels of cement production
357 (Li, 2011; Zhang, 2007). Based on the available data from those field tests, the emission factors are
358 estimated at 0.008, 0.052, and 0.120 g/t-product for cement kilns with FF, ESP, and WET dust
359 collectors, respectively. The data sample for FF passes the statistical test and bootstrap simulation is
360 applied to determine its PDF as a Weibull distribution, as shown in Figure S1(b) in the Supplement.
361 For other dust collectors, however, the current data are too limited and uniform distributions are used,
362 with the lowest and highest measurement values taken as the 10^{th} and 90^{th} percentile of each
363 distribution, respectively.

364 Combining the inter-annual trends of APCD penetration for the sector (Lei et al., 2011; Zhao et
365 al., 2013), the national average emission factor is estimated to have declined from 0.06 in 2005 to
366 0.018 g/t in 2012 (Figure 1(c)), resulting mainly from the sharply increased use of precalciner kilns
367 with FF. For the future, all kilns other than precalciner ones are expected to be closed by 2020 in S1
368 and S2, and by 2030 in S0. In addition, SCR systems are assumed to be deployed at all precalciner
369 kilns in S2 (Zhao et al., 2014). These improvements would lead to reductions in the sector-average
370 EFs to 0.013, 0.012, and 0.008 g/t-product in S0, S1, and S2, respectively, in 2030. Regarding the
371 emissions from coal combustion in cement production, the Hg removal efficiencies for various
372 APCDs are applied to generate the emission factors, and the national average value is estimated to
373 have declined from 0.11 to 0.08 g/t-coal during 2005-2012. While no significant abatement is found
374 for S0 and S1 after 2010, the emission factor would further decrease to 0.04 g/t-coal in S2 by 2030,
375 attributed to the greater use of SCR in the scenario.

Other industrial sources

The emission factors of industrial and heating boilers are estimated using Eq. (3). The Hg release ratios for grate boilers and CFB are estimated at 76% and 91% based on limited domestic measurements (Wang et al., 2000; Tang et al., 2004), lower than those of power plants. Uniform distributions are assumed to quantify the uncertainty of the parameter. WET and CYC are the dominant types of dust collectors for boilers and their removal efficiencies with PDF are assumed to be the same as those for power plants. For the future under S2, FGD is assumed to be deployed at all new boilers, leading to a larger fraction of Hg removal.

Production of polyvinyl chloride polymer (PVC) is a significant contributor to Hg emissions due to wide use of mercuric chloride catalyst in acetylene-making processes. The emission factor is calculated as the product of the Hg content in PVC and its atmospheric release ratio during the production process. In this work, the Hg content in PVC is estimated to range from 0.12 to 0.20 kg Hg/t-PVC, based on investigation by Hao et al. (2005), and the release ratio to be 1%, according to THU (2009). For other processes including Hg mining, production of batteries and fluorescent lamps, large-scale gold production, and oil and gas combustion, the emission factors from AP-42 (USEPA, 2002a) and previous inventory work (Streets et al., 2005) are used due to lack of updated information from domestic measurements. Lognormal distributions are assumed with the CV conservatively set at 100%.

Residential sources

For residential coal consumption, the determination of Hg emission factors is similar to that of industrial boilers. Biomass combustion in this work takes account of crop residues (used as biofuel in households and as waste burned in open fields) and fuel wood (used in households). Domestic information and field measurements (Huang et al., 2011; Zhang et al., 2013) are adopted in this work

399 to estimate the emission factors, and uniform distributions are assumed reflecting the relatively high
400 uncertainty. Based on the domestic dataset, the average EFs for combustion of crop residues (16.7
401 ng/g) and fuel wood (12.3 ng/g) calculated in this work are lower than the values adopted in previous
402 literature (e.g., 37 ng/g for crop residues and 20 ng/g for fuel wood, Streets et al., 2005).

403 Hg emissions from solid waste incineration (SWI) are estimated separately for municipal solid
404 waste incineration (MSWI) and rural household waste incineration (RHWI), due to different mercury
405 content levels and burning techniques. For MSWI, an emission factor of 0.22 g/t with Weibull
406 distribution is estimated, with bootstrap simulation based on domestic field tests by L Chen et al.
407 (2013) and Hu et al. (2012) (Figure S1(c) in the Supplement). The emission factor for RHWI is
408 estimated as the product of Hg content and the atmospheric release ratio, which are obtained from Hu
409 et al. (2012).

410 **3.2 Speciation of Hg with probability distribution functions**

411 Understanding speciation of Hg plays a crucial role in understanding its transport and chemical
412 cycling, which depends significantly on the chemical form. The fate of Hg released to atmosphere
413 varies by species (Hg^0, Hg^{2+}, and Hg^p), which in turn are determined by fuel quality and the removal
414 mechanisms of APCDs, thereby varying significantly by emission source. In this work, a thorough
415 review of existing studies is conducted to compile a database of Hg speciation by sector, and thus to
416 provide the mass fractions of the three main chemical forms (see details in Table S4 in the
417 Supplement). In general, the emission sources that determine Hg speciation can be divided into three
418 categories, according to the nature of APCD deployment and data availability. First are those sources
419 whose emission factors can be calculated based on the removal efficiencies of different APCD (e.g.,
420 CPP, CEM, ISP, OIB and RC), in which case the mass fractions are estimated based on results from
421 field measurements by type of APCD. Second are sources with insufficient measurement samples to

422 determine emission factors by APCD, in which case the average values of available field test results
423 are calculated and directly applied as the mass fractions of the three species for the sector (e.g., NMS,
424 BIO and SWI). Third are sources for which very little domestic information about speciation can be
425 found, in which case results from global studies (Pacyna and Pacyna, 2002) have to be used, with
426 little update to previous inventories (Streets et al., 2005). Those sources mainly include industrial
427 processes like artisanal gold production, Hg mining, and battery and fluorescent lamp production.
428 As shown in Table S4, the speciation of total Hg varies considerably by different types of APCD
429 configurations. For example, the Hg^0 mass fraction averaged over all estimates in the literature is 83%
430 for ESP+FGD, attributed to the relatively strong removal effects of both ESP and FGD on Hg^{2+} and
431 Hg^p. Inclusion of SCR leads to significant increase in the Hg^{2+} fraction, resulting mainly from the
432 conversion of Hg^0 to Hg^{2+} by the SCR process (Wang et al., 2010b). In general, oxidation of Hg^0
433 leads to higher removal of Hg because Hg^{2+} is more liable to be adsorbed in FGD scrubber solution,
434 and use of advanced dust collectors leads to lower Hg^p as most of it can be captured on particles.
435 For mass fraction data that pass the Kolmogorov-Smirnov test, bootstrap simulation is applied to
436 determine a PDF, e.g., the mass fractions of Hg^{2+} for ESP, ESP+FGD and SCR+ESP+FGD (Figure
437 S1(d)-(f) in the Supplement). Otherwise, triangular or uniform distributions are tentatively applied.
438 The PDFs for Hg speciation are summarized in Table 2.
439

440 **4 RESULTS AND DISCUSSION**

441 **4.1 Historical trends in mercury emissions to the atmosphere**

442 The total national emissions of anthropogenic Hg are estimated to have increased from 679.0 t in
443 2005 to 749.8 t in 2012, with a peak of 770.6 t in 2011, as shown in Figure 3. The annual growth rate

444 of emissions averaged 1.4% during 2005-2012, much lower than that of China's energy consumption
445 (7.6%) or the economy (>10%). The result reflects effective constraints on Hg emissions since 2005,
446 compared to relatively fast growth in early 2000s (e.g., 8% annual growth of Hg emissions from 2000
447 to 2003 suggested by Wu et al. (2006)), and may help to explain decreased observed Hg
448 concentrations worldwide. This national trend, however, is currently difficult to confirm fully with
449 field observations, given the lack of long-term monitoring data for atmospheric ambient Hg in either
450 polluted cities or background regions. Limited inter-annual results for one background area (Changbai
451 Mountain in northeastern China) show reduced Hg levels (Wan et al., 2009; Fu et al., 2012b), but
452 those differences are believed to result from changes in sampling location rather than emissions
453 (personal communication with X. Fu of the Institute of Geochemistry, Chinese Academy of Sciences,
454 2014). The speciation of Hg emissions is relatively stable for recent years, with the mass fractions of
455 around 55%, 39%, and 6% for Hg^0, Hg^{2+}, and Hg^p, respectively.

456 The annual emissions by source category are summarized in Table 3. Coal combustion, gold
457 mining, and nonferrous metal smelting are the largest sources of anthropogenic Hg, accounting
458 together for 85% of national total emissions. The share of coal combustion (from the power sector,
459 industrial and heating boilers, cement kilns, residential stoves, and iron & steel production, in
460 declining order) to total national emissions is estimated to have increased from 43% in 2005 to 49%
461 in 2012. This is mainly due to relatively constant emission levels of gold mining and nonferrous metal
462 sectors during the same period, resulting from penetration of newer and more advanced mining and
463 manufacturing technologies. Emissions of Hg^0, Hg^{2+} and Hg^p are summarized by sector in Table
464 S5-S7 of the Supplement. For Hg^0 and Hg^{2+}, the three biggest sources are the same as those for total
465 Hg emissions, i.e., coal combustion, gold mining, and nonferrous metal smelting. For Hg^p, coal

466 combustion plays a dominant role, with the share ranging 78%-84% for various years, as very little
467 Hg^p emissions are estimated from gold mining, zinc smelting, and lead smelting in this work.
468 Provincial emissions, including inter-annual variations, are assessed and illustrated in Figure 4.
469 Because of uncertainties about both emission levels and spatial distribution, Hg emissions from
470 ASGM are omitted from the provincial analysis. While coal combustion is unsurprisingly identified as
471 the biggest source of atmospheric Hg in most provinces, relatively high emissions from
472 non-combustion sources are estimated for several provinces including Hunan, Yunnan, Henan,
473 Guangxi, Anhui, and Shaanxi, resulting mainly from the large production of Zn and/or Pb in those
474 regions. Clear differences in emission trends from 2005 to 2012 are found by region. In contrast to
475 most provinces that have seen increasing emissions, the three regions with the highest densities of
476 population, economic activity, and other pollution show declining estimated emissions, i.e., the
477 Jing-Jin-Ji region (JJJ, including Beijing, Tianjin and Hebei), the Yangtze River Delta region (YRD,
478 including Shanghai, Jiangsu and Zhejiang), and the Pearl River Delta region (PRD, including
479 Guangdong). The collective share of total Hg emissions of the 7 provinces in these regions is
480 estimated to have declined from 24% in 2005 to 19% in 2012, which is similar to trends in criteria air
481 pollutants (Zhao et al., 2013). On one hand, this regional deviation indicates slower growth in heavily
482 polluting industry and the progress of emission controls in highly developed regions. On the other
483 hand, it indicates that China's air pollution challenges have been expanding to less developed interior
484 provinces, which are experiencing rapid urbanization, accelerated economic development, and fast
485 growth of pollution sources.
486 To be applicable to simulation of atmospheric transport and chemistry, annual Hg emissions at
487 the provincial level are allocated to a $0.25^o \times 0.25^o$ grid system, applying the methods described in
488 Zhao et al. (2012). Note the emissions from production of coal-fired power, cement, and iron & steel

489 are allocated at the unit or plant level (e.g., Figure S2(a) in the Supplement for coal-fired power
490 plants). Shown in Figure S2(b)-(d) are the gridded emissions of China's anthropogenic Hg^0, Hg^{2+} and
491 Hg^p, respectively.

492 **4.2 Implication of emission controls on national Hg emissions**

493 Rather than continuing swift, economy-driven grown, China's anthropogenic Hg emissions have
494 slowed since 2005, reflecting the success of national strategies in broader emission control. While
495 collectively causing this national trend, emission trends by sector have varied greatly due to different
496 driving factors and uneven control policies. More detailed analysis is thus needed to disentangle the
497 sources contributing most to the Hg emission trends. Particularly high uncertainty undermines
498 estimation of emissions from ASGM, due to scarcity of input data and information, and its annual
499 emission level is assumed unchanged over time in this work. Although recognized as the biggest
500 contributor of the individual sources to total Hg emissions (Table 3), ASGM must unfortunately be
501 omitted here as a source type affecting the national emission trend due to these data constraints.

502 We divide the remaining anthropogenic sources into three categories, as indicated in Figure 5(a).
503 The first category includes sources for which uniform and unchanged emission factors are applied
504 over time (i.e., large-scale gold mining (LGM), biofuel use/biomass open burning (BIO), solid waste
505 incineration (SWI), and other miscellaneous processes (OMP)). The inter-annual variability of Hg
506 emissions from those sources are thereby only affected by the changes of activity levels, and the
507 annual emissions for Category 1 sectors have continued to increase, from 80.3 t in 2005 to 109.8 t in
508 2012. Due to their relatively small fraction of total emissions (<15%), however, the Category 1
509 sectors have little influence on the trend of the national total, which shows much slower growth and
510 even reduced emissions in a few years, as shown in Figure 5(a). Category 2 consists of coal
511 combustion for heating (HB), other industrial boilers (OIB), and residential use (RC and ROG), those

512 for which emission factors are region-dependent and show little inter-annual variation due to very
513 limited implementation of pollution control measures. The Hg emission trend of these sources
514 therefore depends mainly on the intensive coal use in recent years, and estimated emissions in 2012
515 are 47% higher than those of 2005. Category 3 includes coal-fired power plants (CPP), cement
516 production (CEM), iron & steel plants (ISP), and nonferrous metal smelting (NMS). Although the
517 activity levels (i.e., coal consumption and industrial production) increased in these sources at similar
518 rates as the sectors of Categories 1 and 2, the Hg emission trends of Category 3 sectors are dominated
519 by the combined effects of improved manufacturing technologies and increased use of APCDs to
520 control criteria air pollutants. The emissions of these sectors are estimated to have peaked at 362 t in
521 2007, and then to have declined to 313 t in 2012, largely offsetting the increase in emissions from
522 Categories 1 and 2 and playing a crucial role in constraining total national emissions.

523 Figure 5(b) compares the trends of activity levels and Hg emissions for Category 3 sectors from
524 2005 to 2012. During the period, coal consumption from production of coal-fired power, cement, steel,
525 and nonferrous metals increased by 70%, 107%, 158%, and 104%, respectively. A leveling of
526 industrial production is found in 2008, attributed to production constraints imposed for the Beijing
527 Olympics and to the economic recession at the end of 2008. However, economic activities increased
528 sharply again under a major economic stimulus policy responding to the recession, and energy and
529 industrial production continued to grow swiftly in the following years. Despite the fast growth of
530 activity levels, however, the Hg emissions from the four sectors were clearly constrained, to varying
531 degrees: those from CEM decreased by 38%, those from CPP and NMS in 2012 returned to the levels
532 of 2005, and only those from ISP increased, by 44%, though still far less than growth of steel
533 production. As described in Section 3, the reduced emission factors through the period are the main
534 reasons for the emission abatement, attributed to the replacement of old and small plants or kilns with

larger ones with high combustion efficiencies and advanced control technologies. The increased penetrations of FGD and SCR systems in CPP, precalciner kilns with FF in CEM, mechanized coking ovens with ESP in ISP,, and improved manufacturing technologies in NMS have lead to great ancillary benefits of atmospheric Hg emission abatement. As indicated in Figure S3 in the Supplement, the emission controls are estimated to have cut 100, 93, 30, and 76 t of Hg emissions in 2012 for CPP, CEM, ISP and NMS, respectively, compared to a hypothetical case in which no progress of emission control is assumed for the four sectors since 2005. Without the controls, the Hg emissions of those sectors in 2012 would have exceeded 600 t, almost double the current estimate. This confirms that China's pollution controls in power and key industrial sectors have greatly slowed national Hg emissions, and that energy consumption and industrial production are poor proxies for Hg emissions.

4.3 Evaluation of the estimated emissions against other studies

There are several global inventories that include data for China, including those by the United Nations Environment Programme (AMAP/UNEP, 2008; 2013; Pacyna et al., 2010), International Institute for Applied System Analysis (IIASA, Rafaj et al., 2013), Emission Database for Global Atmospheric Research (EDGAR, Muntean et al., 2014), and Peking University (Y Chen et al., 2013). The trends in China's Hg emissions estimated in this work is difficult to compare directly to those studies for two main reasons: 1) limited studies have been conducted of China's national total Hg emissions for the most recent years, a period with dramatic changes in emission controls across the country; and 2) the sectors and sources of anthropogenic Hg emissions concerned are not defined similarly in different inventories. For earlier years, Wu et al. (2006) estimated China's anthropogenic Hg emissions increased from 552 in 1995 to 696 t in 2003, with a higher annual growth rate (2.9%) than this work for 2005-2012 (1.4%). The comparison thus again indicates the constraints air

558 pollution control measures have exerted on Hg emissions since 2005, given the continued fast growth
559 of the economy and energy use. The results of speciation analysis are similar between Wu et al. (2006)
560 and this work, with slightly larger mass fraction of Hg^p (12% vs. 6%) but a smaller one of Hg^{2+} (32%
561 vs. 39%) in Wu et al. This is probably due to oxidation of Hg^0 by APCDs and increased use of
562 advanced dust collectors after 2005 considered in this work.

563 Illustrated in Figure 3 are the estimates of China's anthropogenic Hg emissions for various years
564 between 2005 and 2012 from different inventories. (Note that estimates by Y Chen et al. (2013) are
565 not shown because that study included only combustion sources, not all anthropogenic sources.) The
566 emissions estimated in this work are generally larger than those of global inventories, except for the
567 results of UNEP for 2005 (AMAP/UNEP, 2008). In particular, the estimates for 2005-2008 by
568 Muntean et al. (2014) are clearly below the lower bounds of 95% confidence intervals (CI) of this
569 work (see Section 4.4 for details). The elevated estimate in this work is supported by limited
570 top-down studies, e.g., Pan et al. (2007), who applied an inverse modeling method with
571 four-dimensional variational data assimilation and derived a larger Hg^0 emission estimate than those
572 from bottom-up methods. Most recent studies evaluated the annual emissions of China's
573 anthropogenic Hg at 643 t for 2007 (Wang et al., 2014) and 494 t for 2008 (Muntean et al., 2014), i.e.,
574 101 and 248 t smaller than our estimates, respectively. Wang et al. (2014) and Muntean et al. (2014)
575 further applied their emissions in GEOS-Chem model and the simulated ambient total Hg or Hg^0
576 concentrations were generally lower than observation at background/rural sites across the country,
577 implying a possible underestimate of Hg emissions.

578 To better understand the reasons for the discrepancies of various studies, the emissions from
579 particular sectors in global inventories and in this work are summarized and compared in Table S8 in
580 the Supplement. For 2005, the much higher estimates of the UNEP inventory (AMAP/UNEP, 2008;

581 Pacyna et al., 2010) compared to this work result mainly from the enhanced emissions of CPP and the
582 combined HB & OIB sectors in the UNEP inventories. Little consideration of emission controls leads
583 to larger emission factors than those used in this work. For 2010, however, lower emissions of CPP
584 are estimated in the UNEP inventory (AMAP/UNEP, 2013), attributed mainly to both higher
585 penetrations and higher Hg removal efficiencies of APCDs compared to this study. The large
586 differences in emissions from HB & OIB and NMS are the main sources of higher national totals in
587 this work than most of the other global inventories. For example, AMAP/UNEP (2013) uses the
588 energy data from the International Energy Agency, which estimates coal consumption of China's
589 industrial boilers as 110 Mt lower than the official data used here for 2010. FF systems, which are
590 able to capture some Hg emissions, are assumed to be deployed at 25% of Chinese industrial boilers
591 by AMAP/UNEP (2013), while our data indicates a much lower penetration. For NMS, AMAP/UNEP
592 (2013) and Muntean et al. (2014) apply activity data from USGS (2011), which provides lower
593 nonferrous metal production estimates than NBS (2013b). Muntean et al. (2014) uses emission factors
594 from EMEP/EEA (2009), i.e., 5 g/t-Zn, 0.9 g/t-Pb, and 0.03 g/t-Cu, much lower than those derived in
595 this work.

596 Besides the total emissions, several studies have been conducted to analyze the Hg emissions
597 from certain sectors in China. For coal combustion sources as a whole, Tian et al. (2010) calculated
598 the Hg emissions at 284 and 306 t for 2005 and 2007, respectively, within 10% of our estimates. Y
599 Chen et al. (2013) calculated China's Hg emissions from coal combustion at 362 t for 2007, of which
600 the emissions from CPP were 204 t, much larger than our estimate of 152 t. From a global perspective,
601 Y Chen et al. (2013) estimated the penetrations of APCD by country using a parameterized function,
602 and derived relatively low fractions of APCD for the power sector in China. Streets et al. (2009b)
603 calculated the emissions from CPP at 125 t for 2005, while Tian et al. (2012) estimated that annual

604 emissions from CPP during 2005-2007 ranged 135-139 t, with little inter-annual variability. Those
605 estimates are somewhat lower than our results. Although the differences could be attributed to many
606 factors including discrepancies in details regarding boiler technologies and data sources of Hg content
607 of coal, the relatively conservative removal efficiencies of APCDs for Hg assessed and applied in this
608 work (as shown in Figure 2) are believed to be the most important reason for the higher estimate of
609 Hg emissions. Wang et al. (2010c) estimated that Hg emissions from CPP would reach 155 t in 2010,
610 higher than our results. However, the energy data and penetrations of APCDs (especially FGD) in
611 Wang et al. (2010c) were predictions based on Zhao et al. (2008), as the official statistics for 2010
612 were unavailable when the study was conducted. The larger annual coal consumption by CPP and
613 lower penetration of FGDs in the study compared to the official statistics (1735 Mt vs. 1576 Mt, and
614 70% vs. 86%, respectively) could lead to an overestimate of Hg emissions for the sector.

615 For NMS, previous inventories commonly used constant emission factors, citing lack of detailed
616 analyses of the trends in manufacturing technology penetration and thereby any ancillary effects on
617 Hg emissions. Feng et al. (2009) summarized results from previous studies and estimated that the
618 emission factors of NMS in China for 1995-2003 could reach as high as 6-155 g/t-Zn, 44 g/t-Pb, and
619 10 g/t-Cu, while Pirrone et al. (2010) adopted 7 g/t-Zn, 3 g/t-Pb, and 5 g/t-Cu for a 2003 emission
620 estimate for China, based on results from developed countries. If those two sets of EF values are
621 applied ignoring possible variation over time, Hg emissions from NPS in 2012 would be 475 t and 80
622 t, i.e., 420% larger and 12% lower than this work, respectively. The big gaps between different
623 estimates, as indicated in Figure 6(a), reveal the importance of better tracking the inter-annual trends
624 of emission factors for the sector. Based on a detailed survey on individual smelting plants, a more
625 recent study by Wu et al. (2012) developed a technology-based methodology with consideration of
626 smelting processes, mercury concentrations in ore concentrates, and mercury removal efficiencies of

627 APCDs. They calculated that emissions declined from 87 in 2005 to 72 t in 2010, more consistent
628 with our study than those using constant emission factors.

629 For ISP and CEM, emission factors in previous inventories were mainly obtained from Pacyna
630 and Pacyna (2002) and Streets et al. (2005), respectively, i.e., 0.04 g/t-product. With these uniform
631 emission factors adopted, estimated Hg emissions from the two sectors during 2005-2012 would
632 continue increasing from 15 to 38 and 43 to 88 t, respectively, as shown in Figure 6 (b) and (c). This
633 plainly ignores the effects of improved manufacturing technologies and increased use of APCDs, and
634 would potentially overestimate emissions, particularly in recent years. For MSWI, the emission factor
635 of 2.8 g/t from UNECE/EMEP (2004) was widely accepted in previous inventories. A series of
636 domestic field measurements, however, suggested a much smaller value of 0.22 g/t for China (L Chen
637 et al., 2013; Hu et al. 2012), and lower emissions are also estimated in this work (Figure 6(d)). Given
638 the swift growth of solid wastes in China, more field tests on both municipal and rural solid waste
639 burning plants are thus imperative to confirm the levels of emission factors and to reduce the
640 uncertainties of Hg emission estimates for these sources.

641 **4.4 Uncertainties of national emission inventory**

642 The uncertainties of anthropogenic Hg emissions in China for 2005-2012 are quantified using
643 Monte-Carlo simulation and the results for selected years are summarized in Table 4. In 2010, for
644 example, the uncertainties of total Hg emissions and those from coal combustion are estimated at
645 -23%–+51% (95% CI) and -49%–+69%, respectively. Since the annual emissions from ASGM and
646 associated uncertainties are assumed to be unchanged during the period and are thus comparatively
647 subjective, the uncertainties of anthropogenic Hg emissions excluding ASGM is further calculated, at
648 -23%–+61% (95% CI). The uncertainties of the current Hg emission inventory are believed to be
649 partly responsible for the differences in ambient Hg levels between observations and model

650 simulations (e.g., a 0-50% difference suggested by Wang et al., 2014). Larger uncertainties are found
651 for individual Hg species than for total Hg, e.g., -31%–+58%, -32%–+69%, and -51%–+114% (95%
652 CIs) for Hg^0, Hg^{2+}, and Hg^p in 2010, respectively (not shown in the table). Among the three aggregate
653 sectors (CPP, IND, and RES), the uncertainties of IND are relatively small. This does not imply that
654 the emission characteristics of IND are well understood, however, but rather results from the
655 aggregation of the uncertainties of all industrial sources. It thus cannot reflect larger uncertainties for
656 particular IND sources.

657 Figure S4 illustrates the emission estimates and uncertainties by source for different Hg species
658 in 2010. For all species, biomass burning (BIO), solid waste incineration (SWI) and residential oil &
659 gas burning (ROG) are the sources with the largest estimated uncertainty relative to their central
660 estimates (i.e., 95% CIs expressed in percentages). It is nevertheless particular industrial sources,
661 including those with less relative uncertainty, that are greater determinants of the national Hg
662 emission uncertainty, because of their large fractions of total emissions. Those sources include
663 coal-fired power plants (CPP) for Hg^0, nonferrous metal smelting (NMS) and gold mining (GM) for
664 Hg^0 and Hg^{2+}, and industrial and residential coal burning (OIB and RC) for Hg^p.

665 Table 5 summarizes the parameters that are most significant in determining the uncertainties of
666 emissions according to their contributions to the variance of emissions. In most cases, parameters
667 related to emission factors contribute most to the uncertainties, including the Hg content of coal in
668 provinces with large consumption (e.g., Shandong and Henan), emission factors of biomass burning
669 and particular technologies for nonferrous metal smelting, and the removal efficiencies of dominant
670 APCDs. The amount of burned coal and biomass are found to be important specifically to the
671 emission uncertainty of the residential sector. For individual species, the mass fractions of different
672 species for various APCDs and gold mining are identified as key determinants of uncertainty.

673 It should be noted that no inter-annual variation for those parameters related to emission factors
674 is assumed for the research period, even if large uncertainty exists for them in a given year. Thus each
675 individual parameter or emission factor applied for estimation of emission uncertainties for a given
676 year is statistically correlated with it for another year in the Monte-Carlo simulation framework.
677 Under this ideal assumption, the uncertainties in emissions for an individual year, whether big or
678 small, are not associated with the inter-annual trends in emissions.

679 Inclusion of more results from recent measurements of emission factors reduces the uncertainty
680 of CPP for 2005 estimated here compared to that estimated for 2003 by Wu et al. (2003). It can be
681 seen from Table 4, however, that the uncertainties of emissions from CPP increased from 2005 to
682 2012. This results mainly from the fast penetration of FGD systems after 2005 and that of SCR after
683 2010, of which the ancillary effects on Hg control varied significantly among measured plants. In past
684 years, installed FGD systems were believed to be operated sporadically, in order to save operational
685 costs, and large discrepancies in estimated SO_2-removal efficiencies exist across the country (Xu,
686 2011; Zhao et al., 2013; 2014). The unclear operation of FGD causes a wide range of estimated Hg
687 removal efficiencies of the systems and thus enhances the uncertainties of the emission estimate, as
688 FGD increasingly dominates the sector over the study period. In addition, the Hg removal effects of
689 SCR are still poorly quantified, and the uncertainties of Hg emissions are further elevated in recent
690 years because China is currently undertaking NO_X control largely through expanded use of SCR
691 (Zhao et al., 2014). As shown in Figure 7, the contribution of Hg removal efficiency of FGD to the
692 variance of CPP emissions increases from 0% in 2005 to 26% in 2010, and it has been the most
693 important parameter contributing to the uncertainty of CPP emissions since 2009. In 2012, Hg
694 removal efficiencies of FGD and SCR are estimated to collectively contribute 37% of the uncertainty
695 of Hg emissions. The emission uncertainties of given industrial sources increased recently for similar

696 reasons. The uncertainty of Hg emissions from NMS, for example, increased from -46%–+116% in
697 2005 to -45%–+169% in 2012. This is attributed mainly to the increased use of electrolytic processes
698 in Zinc smelting, for which domestic measurements are rare and the emission factor has high
699 uncertainty. Moreover, the reduced ratios of gold extraction by amalgamation, reported but
700 unconfirmed, enhance the Hg emission uncertainty of gold mining. In general, therefore, the
701 uncertainty of Hg emissions is higher in the most recent years and may continue to be so in the near
702 future. More field tests or investigations of particularly important sectors are needed for better
703 understanding of the evolution of emission sources and their benefits to Hg control.

704 **4.5 Future emission trends by scenarios**

705 The projected national emissions through 2030 are summarized by sector in Table 6. As shown
706 in Figure 3 and Table 6, China's anthropogenic Hg emissions are likely to increase slightly in the
707 future, even with a few new Hg-specific control measures, judged by S0 and S1 in this work. The
708 emissions in 2030 for the two scenarios are estimated at 869 and 813 t, i.e., 16% and 8% higher than
709 2012, respectively. The estimated growth in Hg emissions continues to be far slower than that of the
710 economy and energy consumption projected by IEA (2012). This results mainly from the ancillary
711 benefits of ongoing control policies targeting other pollutants in the country, such as the National
712 Action Plan for Air Pollution Prevention and Control (Zhao et al., 2014). These policies will ensure
713 continued deployment of advanced technologies with improved energy efficiencies and air pollutant
714 removal rates across numerous economic sectors. The results clearly suggest that projecting China's
715 Hg trajectory based simply on economic and/or energy growth would likely lead to overestimation.
716 Comparing the three scenarios, S2 produces a much larger reduction in Hg emissions over S0
717 than does S1. This suggests that implementation of Hg-specific controls may offer more effective
718 emission reduction than relying on the ancillary benefits of energy conservation. In particular, if key

719 industrial sources including ASGM can be controlled by national regulations (two thirds of such
720 emissions are assumed to be cut in S2, based on an estimate by Feng et al. (2009)), the national Hg
721 emissions from 2015 on would be less than those of 2005, and by 2030 would be less than 600 t, 23%
722 below the 2012 total. For industrial sources other than metallurgy, however, the Hg abatement in S2 is
723 relatively modest, implying small future ancillary effects on Hg of APCDs due to their nearly
724 saturated deployment in most sectors. Expanded use of Hg-specific removal devices in sectors such as
725 power generation and heavy industry is thus essential to further reduce Hg emissions in the future. In
726 addition, very few effective policies are identified that target residential sources, resulting in elevated
727 emissions for the sector. The RES share of total anthropogenic Hg emissions in S2 is thus projected to
728 rise from 11% in 2012 to 19% in 2030.
729

730 **5 CONCLUSIONS**

731 Facing difficult challenges of severe urban and regional air pollution driven by swift economic
732 development and enormous energy consumption, China has been implementing a series of policies in
733 energy conservation and emission control since 2005. Although not specifically targeting Hg, a
734 pollutant of broad international concern, the policies and measures are judged to have effectively
735 constrained China's Hg emissions because of their ancillary effects. From 2005 to 2012, China's
736 anthropogenic emissions of atmospheric Hg are estimated to have increased from 679 to 750 t, a
737 much slower rate of growth than those of China's economy and energy consumption. In particular,
738 decreased Hg emissions are estimated for the JJJ, YRD, and PRD regions, the areas of the country
739 with the highest density of population, economic activity, and energy consumption. Applying
740 improved methods for emission estimation, almost half of the collective Hg emissions from four key

741 sectors (power generation, cement production, iron & steel production, and nonferrous metal smelting)
742 are estimated to have been abated from 2005 to 2012, attributed to the enhanced use of devices with
743 high energy efficiencies and pollutant removal rates. Even with considerable growth of energy use
744 projected by IEA (2012), continued measures in pollution control will further constrain the national
745 Hg emission trajectory in the future. Analyses that overlook the effects of recent energy and pollution
746 control policies will thus likely result in overestimation of China's recent and future Hg emissions.
747 It should be noted, however, that the uncertainties of China's Hg emission estimate have at the
748 same time increased in recent years. This is mainly because of high uncertainties about the operational
749 and other characteristics of the same advanced APCDs or improved manufacturing technologies that
750 are nevertheless believed to be reducing emissions in key sectors. In addition, the unknown levels and
751 locations of illegal ASGM activities continue to contribute significantly to the uncertainty of China's
752 Hg emissions. Beyond interest in the national Hg emission totals, the relatively poor understanding of
753 the speciation of Hg by sector elevates the uncertainties of emissions of different species, which are of
754 particular importance to scientists simulating atmospheric transport, chemistry, and the environmental
755 fate of Hg. Given the ongoing dramatic changes of emission sources under current policies within the
756 country, therefore, systematic investigations by sector are suggested for Hg pollution, to better track
757 the variability of emission levels and efficiently reduce the uncertainty of emissions for all Hg species.
758 Middle- to long-term observations of atmospheric Hg, both in polluted urban and regional background
759 areas, are also needed to validate analyses of China's anthropogenic Hg emission and to confirm the
760 beneficial effects of pollution control implementation in the country.
761

ACKNOWLEDGEMENT

This work was sponsored by the Natural Science Foundation of China (41205110), Natural Science Foundation of Jiangsu (BK20140020 and BK2012310). We would like to thank Shuxiao Wang and Qingru Wu from Tsinghua University for providing detailed technology information on non-ferrous metal smelting, Simon Wilson from the Arctic Monitoring and Assessment Programme for providing information and data on emissions from artisanal gold mining, and Shigeru Suehiro from the International Energy Agency for providing data for Chinese energy and industrial projections. Thanks also go to three anonymous reviewers for their very valuable comments to improve this work.

REFERENCES

AGC (Artisanal Gold Council), Global Database on Mercury Emissions from Artisanal and Small Scale Mining (ASGM), 2010. Available at: http://www.mercurywatch.org

AMAP/UNEP, 2013. Technical Background Report for the Global Mercury Assessment 2013. Arctic Monitoring and Assessment Programme, Oslo, Norway/UNEP Chemicals Branch, Geneva, Switzerland, 263 pp.

AMAP/UNEP, 2008. Technical Background Report to the Global Atmospheric Mercury Assessment. Arctic Monitoring and Assessment Programme, Oslo, Norway/UNEP Chemicals Branch, Geneva, Switzerland, 159 pp.

Chen, C., Wang, H., Zhang, W., Hu, D., Chen, L., Wang, X.: High-resolution inventory of mercury emissions from biomass burning in China for 2000-2010 and a projection for 2020, J. Geophys. Res., 118, 12248-12256, 2013.

Chen, L., Liu, M., Fan, R., Ma, S., Xu, Z., Ren, M., He, Q.: Mercury speciation and emission from municipal solid waste incinerators in the Pearl River Delta, South China. Sci. Total Environ., 447, 396-402, 2013.

787 Chen, Y., Wang, R., Shen, H., Li, W., Chen, H., Huang, Y., Zhang, Y., Chen, Y., Su, S., Lin, N., Liu,
788 J., Li, B., Wang, X., Liu, W., Coveney, R. M., and Tao, S.: Global mercury emissions from
789 combustion in light of international fuel trading, Environ. Sci. Technol., 48, 1727-1735, 2013.

790 China Association of Urban Environmental Sanitation (CAUES): Development Report on China
791 Urban Environmental Sanitation (2012), China City Press, Beijing, 2013 (in Chinese).

792 Ci, Z., Zhang, X., Wang, Z.: Enhancing atmospheric mercury research in China to improve the
793 current understanding of the global mercury cycle: the need for urgent and closely coordinated efforts,
794 Environ. Sci. Technol., 46, 5636-5642, 2012.

795 Corbitt, E. S., Jacob, D. J., Holmes, C. D., Streets, D. G., Sunderland, E. M.: Global source–receptor
796 relationships for mercury deposition under present-day and 2050 emissions scenarios, Environ. Sci.
797 Technol., 45, 10477-10484, 2011.

798 Cui, X., Ma, L. P., Deng. C. L., Xu. W. J., Mao. N.: Research progress of removing mercury from
799 coal-fired flue gas, Chemical Industry and Engineering Progress, 30, 1607-1612, 2011(in Chinese).

800 Driscoll, C. T., Mason, R. P., Chan, H. M., Jacob, D. J., and Pirrone, N.: Mercury as a global pollutant:
801 sources, pathways, and effects. Environ. Sci. Technol., 47, 4967-4983, 2013.

802 EMEP/EEA: EMEP/EEA CORINAIR emission inventory guidebook. Technical report No. 9/2009.
803 European Environment Agency, 2009. Available at:
804 http://www.eea.europa.eu/publications/emep-eea-emission-inventory-guidebook-2009

805 Feng, X., Streets, D. G., Hao, J., Wu, Y., Li, G.: Mercury emissions from industrial sources in China,
806 In Pirrone, N., Mason, R. P. (Eds): Mercury Fate and Transport in the Global Atmosphere, Springer
807 US, 67-79, 2009.

808 Feng, X., Li, G., Qiu, G.: A preliminary study on mercury contamination to the environment from
809 artisanal zinc smelting using indigenous methods in Hezhang county, Guizhou, China-Part 1: mercury
810 emission from zinc smelting and its influences on the surface waters, Atmos. Environ., 38, 6223-6230,
811 2004.

812 Feng, X., Sommer, J., Lindqvist, O., Hong, Y.: Occurrence, emissions and deposition of mercury
813 during coal combustion in the province Guizhou, China, Water Air Soil Pollut., 139, 311-324, 2002.

814 Frey, H. C., Zheng, J. Y.: Quantification of variability and uncertainty in air pollutant emission
815 inventories: method and case study for utility NO_X emissions, J. Air & Waste Manage. Assoc., 52,
816 1083-1095, 2002.

817 Fu, X., Feng, X., Sommar, J., Wang, S.: A review of studies on atmospheric mercury in China, Sci.
818 Total Environ., 421-422, 73-81, 2012a.

819 Fu, X., Feng, X., Shang, L., Wang, S., Zhang, H.: Two years of measurements of atmospheric total
820 gaseous mercury (TGM) at a remote site in Mt. Changbai area, Northeastern China, Atmos. Chem.
821 Phys., 12, 4215-4226, 2012b.

822 Guo, Y., Yan, N., Yang, S., Qu, Z., Wu Z., Liu, Y., Liu, P., Jia, J.: Conversion of elemental mercury
823 with a novel membrane delivery catalytic oxidation system, Environ. Sci. Technol., 45, 706-711,
824 2011.

825 Hao, C., Shen, Y., Zhang, Y.: Study on mercury consumption reduction plans for PVC resin industry
826 in China, Research of Environmental Sciences, 18, 112-115, 2005 (in Chinese).

827 Hong, B., Zhu, Y., Feng, X., Wang, Y.: Distribution of mercury in coal gas generating procedure,
828 Earth and Environment, 32, 12-16, 2004 (in Chinese).

829 Hu, D., Zhang, W., Chen, L., Chen, C., Ou, L., Tong, Y., Wei, W., Long, W., Wang, X.: Mercury
830 emissions from waste combustion in China from 2004 to 2010, Atmos. Environ., 62, 359-366, 2012.

831 Huang, W., Yang, Y.: Mercury in coal in China. Coal Geology of China, 14(S), 37-40, 2002 (in
832 Chinese).

833 Huang, X., Li, M., Friedli, H. R. Song, Y., Chang, D., Zhu, L.: Mercury emissions from biomass
834 burning in China, Environ. Sci. Technol., 45, 9442-9448, 2011.

835 Huang, Y., Jin, B., Zhong, Z., Xiao, R.: Study on the distribution of trace elements in gasification
836 products, Proceedings of the CSEE, 24, 208-212, 2004 (in Chinese).

837 International Energy Agency (IEA): World Energy Outlook 2012, International Energy Agency, Paris,
838 France, 2012

839 Ito, S., Yokoyama, T., Asakura, K.: Emissions of mercury and other trace elements from coal-fired
840 power plants in Japan, Sci. Total Environ., 368, 397-402, 2006.

841 Lei, Y., Zhang, Q., Nielsen, C. P., He, K. B.: An inventory of primary air pollutants and CO_2
842 emissions from cement industry in China, 1990–2020, Atmos. Environ., 45, 147-154, 2011.

843 Li, G., Feng, X., Li, Z., Qiu, G., Shang, L., Liang, P., Wang, D., Yang, Y.: Mercury emission to
844 atmosphere from primary Zn production in China, Sci. Total Environ., 408, 4607-4612, 2010.

845 Li, G., Feng, X., Li, Z.: Atmospheric mercury emissions from retort Zn productions, J. Tsinghua Univ.
846 (Sci & Tech), 49, 2001-2004, 2009 (in Chinese).

847 Li, P., Feng, X., Qiu, G., Shang, L., Wang, S.: Mercury pollution in Wuchuan mercury mining area,
848 Guizhou, Southwestern China: The impacts from large scale and artisanal mercury mining, Environ.
849 Int., 42, 59-66, 2012.

850 Li, P., Feng, X., Qiu, G., Shang, L., Wang, S., Meng, B.: Atmospheric mercury emission from
851 artisanal mercury mining in Guizhou Province, Southwestern China, Atmos. Environ., 43, 2247-2251,
852 2009.

853 Li, W.: Characterization of Atmospheric Mercury Emissions from Coal-fired Power Plant and Cement
854 Plant (Master Thesis), Xi'nan University, Chongqing, China, 2011 (in Chinese).

855 Lin, C.-J., Pan, L., Streets, D. G., Shetty, S. K., Jang, C., Feng, X., Chu, H.-W., and Ho, T. C.:
856 Estimating mercury emission outflow from East Asia using CMAQ-Hg, Atmos. Chem. Phys., 10,
857 1853-1864, 2010.

858 Muntean, M., Jassens-Maenhout, G., Song, S., Selin, N. E., Olivier, J. G. J., Guizzardi, D., Maas, R.,
859 and Dentener, F.: Trend analysis from 1970 to 2008 and model evaluation of EDGARv4 global
860 gridded anthropogenic mercury emissions, Sci. Total Environ., 494-495, 337-350, 2014.

861 National Bureau of Statistics (NBS): China Statistical Yearbook 2005-2012, China Statistics Press,
862 Beijing, 2013a (in Chinese).

863 National Bureau of Statistics (NBS): China Industry Economy Statistical Yearbook 2005-2012, China
864 Statistics Press, Beijing, 2013b (in Chinese).

865 National Bureau of Statistics (NBS): China Statistical Yearbook 2005-2012, China Statistics Press,
866 Beijing, 2013c (in Chinese).

867 Pacyna, E. G., Pacyna, J. M., Sundseth, K., Munthe, J., Kindbom, K., Wilson, S., Steenhuisen, F.,
868 Maxson, P.: Global emission of mercury to the atmosphere from anthropogenic sources in 2005 and
869 projections to 2020, Atmos. Environ., 44, 2487-2499, 2010.

870 Pacyna, E. G., Pacyna, J. M.: Global emission of mercury from anthropogenic sources in 1995, Water
871 Air Soil Pollut., 137, 149-165, 2002.

872 Pan, L., Carmichael, G. R., Adhikary, B., Tang, Y., Streets, D. G., Woo, J. -H., Friedli, H. R., Radke,
873 L. F.: A regional analysis of the fate and transport of mercury in East Asia and an assessment of major
874 uncertainties, Atmos. Environ., 42, 1144-1159, 2008.

875 Pan, L., Chai, T., Carmihael, G. R., Tang, Y., Streets, D., Woo, J. -H., Friedli, H. R., Radke, L. F.:
876 Top-down estimate of mercury emissions in China using four-dimensional variational data
877 assimilation, Atmos. Environ., 41, 2804-2819, 2007.

878 Pirrone, N., Mason, R. P. (Eds): Mercury fate and transport in the global atmosphere, Springer US,
879 2009.

880 Pirrone, N., Cinnirella, S., Feng, X., Finkelman, R. B., Friedli, H. R., Leaner, J., Mason, R.,
881 Mukherjee, A. B., Stracher, G. B., Streets, D. G., Telmer, K.: Global mercury emissions to the
882 atmosphere from anthropogenic and natural sources, Atmos. Chem. Phys, 10, 5951-5964, 2010.

883 Rafaj, P., Bertok, I., Cofala, J., and Schopp, W.: Schopp, W.: Scenarios of global mercury emissions
884 from anthropogenic sources, Atmos. Environ., 79, 472-479, 2013.

885 Slemr, F., Brunke, E. G., Ebinghaus, R., Kuss, J.: Worldwide trend of atmospheric mercury since
886 1995, Atmos. Chem. Phys., 11, 4779−4787, 2011.

887 Srivastava, R K., Hutson, N., Martin, B., Princiotta, F., Staudt, J:: Control of mercury emissions from
888 coal-fired electric utility boilers, Environ. Sci. Technol., 40, 1385-1393, 2006.

889 Streets, D. G., Zhang, Q., Wu, Y.: Projections of global mercury emissions in 2050, Environ. Sci.
890 Technol., 43, 2983-2988, 2009a.

891 Streets, D. G., Hao. J., Wang, S., Wu, Y.: Mercury emissions from coal combustion in China, In
892 Pirrone, N., Mason, R. P. (Eds): Mercury Fate and Transport in the Global Atmosphere, Springer US,
893 51-65, 2009b.

894 Streets, D. G., Hao, J., Wu, Y. Jiang, J., Chan, M., Tian, H., Feng, X.: Anthropogenic mercury
895 emissions in China, Atmos. Environ., 39, 7789-7806, 2005.

896 Tang, S., Feng, X., Shang, L., Yan, H., Hou, Y.: Mercury speciation and emissions in the flue gas of a
897 small-scale coal-fired boiler in Guiyang, Research of Environmental Sciences, 17, 74-76, 2004 (in
898 Chinese).

899 Telmer K, Veiga M. World emissions of mercury from artisanal and small scale gold mining. In
900 Pirrone, N., Mason, R. P. (Eds): Mercury Fate and Transport in the Global Atmosphere, Springer US,
901 131-172, 2009.

902 Tian, H., Wang, Y., Cheng, K., Qu, Y., Hao, J, Xue, Z., Chai, F.: Control strategies of atmospheric
903 mercury emissions from coal-fired power plants in China. J. Air Waste Manag. Assoc., 62, 576-58,
904 2012.

905 Tian, H. Z., Wang, Y., Xue, Z. G., Cheng, K., Qu, Y. P., Chai, F. H., Hao, J. M.: Trend and
906 characteristics of atmospheric emissions of Hg, As, and Se from coal combustion in China,
907 1980–2007, Atmos. Chem. Phys., 10, 11905-11919, 2010.

908 Tsinghua University (THU): Improve the Estimates of Anthropogenic Mercury Emissions in China,
909 Technical report, 2009. Available at: http://ww.chem.unep.ch/MERCURY/.

910 United Nations Economic Commission for Europe/The European Monitoring and Evaluation
911 Programme (UNECE/EMEP): Atmospheric Emission Inventory Guidebook, 2004. Available at
912 http://reports.eea.eu.int/EMEPCORINAIR4/en/page002.html

913 U.S. Environmental Protection Agency (USEPA): Compilation of Air Pollutant Emission Factors
914 (AP-42), 2002a. Available at http://www.epa.gov/ttn/chief/ap42/index.html.

915 U.S. Environmental Protection Agency (USEPA): Characterization and management of residues from
916 coal-fired power plants, Interim Report, EPA-600/R-02-083, 2002b.

917 U. S. Geological Survey (USGS): Commodity Statistics and Information, 2011. Available at:
918 http://minerals.usgs.gov/minerals/pubs/commodity.

919 U. S. Geological Survey (USGS): Mercury content in coal mines in China (unpublished data), 2004.

920 Wan, Q., Feng, X., Lu, J., Zheng, W., Song, X., Han, S., Xu, H.: Atmospheric mercury in Changbai
921 Mountain area, northeastern China-Part 1: the seasonal distribution pattern of total gaseous mercury
922 and its potential sources. Environ. Res., 109:201-206, 2009.

923 Wang, F., The control policy for total emission amount of primary pollutants during the 12th Five
924 Year Plan period, presented at the 17th Workshop on SO_2, NO_X, and Hg pollution control technology
925 and $PM_{2.5}$ control and monitoring technology, Hangzhou, China, May 16-17, 2013.

926 Wang, K., Wang, C., Lu, X. D., Chen, J. N.: Scenario analysis on CO_2 emissions reduction potential
927 in China's iron and steel industry, Energy Policy, 35, 2320-2335, 2007.

928 Wang, L., Wang, S., Zhang, L., Wang, Y., Zhang, Y., Nielsen, C., McElroy, M. B., Hao, J.: Source
929 apportionment of atmospheric mercury pollution in China using the GEOS-Chem model, Environ.
930 Pollut., 190, 166-175, 2014.

931 Wang, Q., Shen, W., Ma, Z.: Estimation of mercury emission from coal combustion in China, Environ.
932 Sci. Technol., 34, 2711-2713, 2000

933 Wang, S. X., Zhang, L., Zhao, B., Meng, Y., Hao, J. M.: Mitigation potential of mercury emissions
934 from coal-fired power plants in China, Energy Fuels, 26, 4635-4642, 2012.

935 Wang, S. X., Song, J. X., Li, G. H., Wu, Y., Zhang, L., Wan, Q., Streets, D. G., Chin, C. K., Hao, J.
936 M.: Estimating mercury emissions from a zinc smelter in relation to China's mercury control policies,
937 Environ. Pollut., 158, 3347-3353, 2010a.

938 Wang, S. X., Zhang, L., Li, G. H., Wu, Y., Hao, J. M., Pirrone, N., Sprovieri, F., Ancora, M. P.:
939 Mercury emission and speciation of coal-fired power plants in China, Atmos. Chem. Phys., 10,
940 1183-1192, 2010b.

941 Wang, S. X., Zhang, L., Wu, Y., Ancora, M. P., Yu Zhao, Hao, J. M.: Synergistic mercury removal by
942 conventional pollutant control strategies for coal-fired power plants in China, J. Air & Waste Manage.
943 Assoc., 60, 722-730, 2010c.

944 Wang, W. X.: Analysis of energy consumption and energy saving potential for iron and steel industry,
945 China Steel, 4, 19-22, 2011 (in Chinese).

946 Wu, Q. R, Wang, S. X., Zhang, L., Song, J. X., Yang, H., Meng, Y.: Update of mercury emissions
947 from China's primary zinc, lead and copper smelters, 2000–2010. Atmos. Chem. Phys., 12,
948 11153-11163, 2012.

949 Wu, Y., Streets, D. G., Wang, S. X., Hao, J. M.: Uncertainties in estimating mercury emissions from
950 coal-fired power plants in China, Atmos. Chem. Phys., 10, 2937-2947, 2010.

951 Wu, Y., Wang, S., Streets, D. G., Hao, J., Chan, M., Jiang. J.: Trends in anthropogenic mercury
952 emissions in China from 1995 to 2003, Environ. Sci. Technol., 40, 5312-5318, 2006.

953 Xu, Y.: Improvements in the operation of SO_2 scrubbers in China's coal power plants, Environ. Sci.
954 Technol., 45, 380-385, 2011.

955 Yao, W., Qu, X., Li, H., Fu, Y.: Production, collection and treatment of garbage in rural areas in
956 China, J Environ Health, 26, 10-12, 2009 (in Chinese).

957 Yan, N., Chen, W., Chen, J., Qu, Z., Guo, Y., Yan, S., Jia, J.: Significance of RuO2 modified SCR
958 catalyst for elemental mercury oxidation in coal-fired flue gas, Environ. Sci. Technol., 45, 5725-5730,
959 2011.

960 Zhang, L., Wang, S., Meng, Y., Hao, J.: Influence of mercury and chlorine content of coal on mercury
961 emissions from coal-fired power plants in China, Environ. Sci. Technol., 46, 6385-6392, 2012a.

962 Zhang, L., Wang, S., Wu, Q., Meng, Y., Yang, H., Wang, F., Hao, J.: Were mercury emission
963 factors for Chinese non-ferrous metal smelters overestimated? Evidence from onsite measurements in
964 six smelters, Environ. Pollut., 171, 109-117, 2012b.

965 Zhang, L., Zhuo, Y., Chen, L., Xu X., Chen, C.: Mercury emissions from six coal-fired power plants
966 in China, Fuel Processing Technology., 89, 1033-1040, 2008.

967 Zhang, L.: Research on mercury emission measurement and estimate from combustion resources
968 (Master Thesis), Zhejiang University, Hangzhou, China, 2007 (in Chinese).

969 Zhang, W., Wei, W., Hu, D., Zhu, Y., Wang, X.: Emission of speciated mercury from residential
970 biomass fuel combustion in China, Energy Fuels, 27, 6792-6800, 2013.

971 Zhao, Y., Zhang, J., Nielsen, C. P.: The effects of energy paths and emission controls and standards
972 on future trends in China's emissions of primary air pollutants, Atmos. Chem. Phys., 14, 8849-8868,
973 2014.

974 Zhao, Y., Zhang, J., Nielsen, C. P.: The effects of recent control policies on trends in emissions of
975 anthropogenic atmospheric pollutants and CO_2 in China, Atmos. Chem. Phys., 13, 487-508, 2013.

976 Zhao, Y., Nielsen, C. P., McElroy, M. B., Zhang, L., Zhang, J.: CO emissions in China: uncertainties
977 and implications of improved energy efficiency and emission control, Atmos. Environ., 49, 103-113,
978 2012.

979 Zhao, Y., Nielsen, C. P., Lei, Y., McElroy, M. B., Hao, J. M.: Quantifying the uncertainties of a
980 bottom-up emission inventory of anthropogenic atmospheric pollutants in China, Atmos. Chem. Phys.,
981 11, 2295-2308, 2011.

982 Zhao, Y., Wang, S. X., Nielsen, C. P., Li, X. H., and Hao, J. M.: Establishment of a database of
983 emission factors for atmospheric pollutants from Chinese coal-fired power plants, Atmos. Environ.,
984 44, 1515-1523, 2010.

985 Zhao, Y., Wang, S. X., Duan, L., Lei, Y., Cao, P. F., Hao, J. M.: Primary air pollutant emissions of
986 coal-fired power plants in China: current status and future prediction. Atmos. Environ., 42, 8442-8452,
987 2008.

988 Zhi, G., Xue, Z., Li, Y., Ma, J., Liu, Y., Meng, F., Chai, F.: Uncertainty of flue gas mercury emissions
989 from coal-fired power plants in China based on field measurements, Research of Environmental
990 Sciences, 26, 814-821, 2013 (in Chinese).

FIGURE CAPTIONS

Figure 1. The penetrations of technologies and inter-annual trends of Hg emission factors for typical sources in China for 2005-2012 and S2 through 2030. In each panel, the left vertical axis indicates the percentages of various technologies and right vertical axis indicates the emission factors.

Figure 2. Mercury removal efficiencies of different APCD combinations estimated in this work, compared with other inventory studies.

Figure 3. National total Hg emissions with speciation from 2005 to 2012 and future trends under three scenarios through 2030. The error bars for 2005-2012 indicate the 95% confidence intervals of the annual total emission estimates. Estimates from other inventories are shown as well for comparison.

Figure 4. Provincial Hg emissions in 2010 and the relative changes between 2005 and 2012. The sizes of the pie graphs indicate absolute emissions by source in 2010. Emissions from ASGM are excluded.

Figure 5. (a) Relative changes in Hg emissions of the national total and different source categories, and (b) Relative changes of Hg emissions and activity levels for given sectors (all values normalized to the levels in 2005)

Figure 6. Comparison of current Hg emission estimates to those without updated time-variant emission factors for (a) nonferrous metal smelting, (b) iron & steel production, (c) cement production, and (d) solid waste incineration.

Figure 7. Contribution of different parameters to variance of Hg emissions from CPP during 2005-2012.

TABLES

Table 1 Uncertainties of Hg emission factors for main sources, expressed as the probability distribution functions (PDF).

Parameters		Samples	Distribution	Key characteristics for distribution functions		
				P10[a]/Min[b]	P90[a]/Max[b]	Mean[a]/Most likely[b]
Release rates of boilers for CPP, %						
PC		32	Triangular	89	100	99
Grate		2	Triangular	92	100	96
CFB		3	Triangular	93	100	98
Release rates of boilers for OIB/HB/FOS, %						
Grate		3	Triangular	51	91	76
CFB		1	Triangular	51	100	91
Hg removal efficiency by APCDs for CPP, %						
FF		5	Weibull	21	84	56
ESP		44	Normal	18	23	20
WET		3	Weibull	4	26	13
FGD+ESP		30	Weibull	40	68	57
CYC		3	Uniform	0	14	-
SCR		7	Triangular	10	100	77
CFB+ESP		3	Weibull	18	60	43
Nonferrous metal smelting [c]						
Zinc	EP	6	Triangular	0	45	9
	ISP	3	Uniform	0	140	-
	RZSP	2	Uniform	2	38	-
	AZSP	4	Triangular	4	203	89
Lead	RPSP	2	Uniform	0	1.4	-
	SMP	2	Uniform	0	12	-
Copper	FFSP	2	Uniform	0	0.3	-
	RPSP	2	Uniform	0.1	0.3	-
Cement production						
FF		7	Weibull	0.006	0.011	0.008
ESP		2	Uniform	0.01	0.11	-
WET/CYC		2	Uniform	0.06	0.18	-
Biofuel use/biomass open burning						
Firewood		26	Uniform	0	50	-
Crops		9	Uniform	0	106	-
Waste incineration						
Municipal		29	Weibull	0.21	0.32	0.27
Rural	Release rates	1	Normal	0.37	0.63	0.5
	Hg content	31	Weibull	0.12	1.58	0.6

[a] P10 values mean that there is a probability of 10% that the actual result would be equal to or below the P10 values; P50 mean that there is a probability of 50% that the actual result would be equal to or below the P50 values; and P90 mean that there is a probability of 90% that the actual result would be equal to or below the P90 values.

[b] These values are for the minimum, the most likely, and the maximum values for the triangular distribution function instead of P10, P50, and P90 values, or for the minimum and maximum values for the uniform distribution function instead of P10 and P90 values.

[c] Full names of manufacturing technologies: EP: electrolytic process; ISP: imperial smelting process; RZSP: retort zinc smelting process; AZ: artisanal zinc smelting process; RPSP: rich-oxygen pool smelting process; SMP: sinter machine process; and FFSP: flash furnace smelting process.

Table 2 Uncertainties of mass fractions of Hg speciation for main source categories.

Parameters		Samples	Distribution	Key characteristics for distribution functions / %		
				P10/Min	P90/Max	Mean/Most likely
FF	Hg^0	4	Triangular	4.8	30.6	15.8
	Hg^p	4	Triangular	0.0	34.8	10.8
ESP	Hg^{2+}	20	Normal	27.9	42.4	35.2
	Hg^p	20	Triangular	0.0	3.6	0.22
FGD+ESP	Hg^{2+}	11	Normal	9.8	22.2	16.0
	Hg^p	11	Triangular	0.0	3.7	0.3
WET	Hg^0	2	Uniform [b]	0.0	60.0	-
	Hg^p	2	Uniform [b]	0.0	28.0	-
NOC [a]	Hg^0	-	Uniform [b]	0.0	48.0	-
	Hg^{2+}	-	Uniform [b]	0.0	40.0	-
SCR	Hg^{2+}	6	Triangular	15.7	40.6	27.6
NMS_Zn	Hg^0	3	Triangular	0.0	55.0	29.0
	Hg^p	3	Uniform	0.0	5.0	-
NMS_Pb	Hg^{2+}	2	Triangular	15.0	65.0	40.0
NMS_Cu	Hg^{2+}	2	Uniform	28.0	72.0	-
BIO	Hg^0	25	Weibull	57.3	94.2	76.9
	Hg^{2+}	25	Triangular	0.0	21.7	5.0
SWI	Hg^0	10	Gamma	1.1	33.8	6.2
	Hg^p	10	Gamma	0.1	2.6	0.5

[a] No control device for coal combustion;

[b] Tentatively assumed

1031 **Table 3 National Hg emissions by source category from 2005 to 2012.**

Source category	2005	2006	2007	2008	2009	2010	2011	2012
Coal-fired power plants	**144.7**	**149.5**	**152.5**	**144.2**	**140.6**	**140.0**	**155.8**	**143.6**
Industry	**473.0**	**495.9**	**530.0**	**533.8**	**546.0**	**542.3**	**540.3**	**526.4**
Cement production	64.4	65.8	66.8	59.1	59.4	45.7	40.1	40.0
Coal use	16.1	17.6	18.7	18.0	20.0	20.4	21.5	22.2
Iron & steel plants	26.2	28.0	28.2	29.7	32.3	34.8	36.8	37.6
Heating boilers	18.1	20.5	24.1	26.0	26.3	30.1	32.6	34.5
Other industrial boilers	61.2	66.7	76.0	81.6	83.7	80.6	87.9	87.4
Nonferrous metal smelting	87.4	98.1	114.2	108.1	112.7	117.6	105.1	91.4
Zinc	43.0	49.0	58.3	59.2	63.4	72.2	69.9	68.1
Lead	39.9	45.0	52.4	45.6	45.8	41.9	34.0	22.0
Copper	4.5	4.1	3.4	3.4	3.5	3.5	1.2	1.4
Gold mining	184.4	183.8	183.8	182.3	183.3	179.5	181.0	182.6
Large scale	17.7	17.1	17.1	15.6	16.6	12.8	14.3	15.9
Artisanal and small scale	166.7	166.7	166.7	166.7	166.7	166.7	166.7	166.7
Other miscellaneous processes	31.2	33.1	37.0	47.0	48.4	54.1	56.8	52.9
Mercury mining	16.2	13.5	14.2	23.7	25.3	28.2	28.3	24.0
Battery/fluorescent lamp production	7.6	8.7	9.8	10.9	10.0	10.0	10.0	10.0
PVC production	7.0	8.8	10.7	10.0	10.7	13.6	16.0	16.3
Oil and gas combustion	0.5	2.1	2.3	2.3	2.4	2.4	2.6	2.6
Residential & commercial sector	**61.3**	**59.8**	**61.4**	**63.6**	**67.8**	**70.7**	**74.2**	**79.5**
Coal burning	30.0	28.0	27.2	30.7	33.0	34.9	36.5	38.5
Biofuel use/biomass open burning	10.3	10.5	9.7	9.2	9.4	8.2	8.3	8.4
Solid waste incineration	10.3	10.9	11.4	11.6	12.4	12.8	13.3	15.3
Municipal	1.7	2.5	3.2	3.5	4.4	5.1	5.7	7.9
Rural	8.6	8.4	8.2	8.1	7.9	7.7	7.6	7.4
Oil and gas combustion	10.7	10.4	13.1	12.1	13.0	14.9	16.1	17.4
Total	**679.0**	**705.2**	**743.8**	**741.7**	**754.4**	**753.0**	**770.3**	**749.5**
Total coal combustion	**296.2**	**310.2**	**326.6**	**330.3**	**335.9**	**340.7**	**371.1**	**363.8**

1032

Table 4 Uncertainties of Hg emissions by sector for 2005, 2008, 2010 and 2012, expressed as the 95% confidence intervals of central estimates. The unit for emissions is metric tons (t).

	2005	2008	2010	2012
CPP	145 (-48%, +73%)	144 (-50%, +70%)	140 (-51%, +77%)	144 (-50%, +89%)
IND	473 (-30%, +43%)	534 (-27%, +46%)	543 (-26%, +51%)	527 (-27%, +54%)
RES	61 (-36%, +144%)	64 (-35%, +127%)	71 (-34%, +123%)	79 (-35%, +115%)
Total	679 (-26%, +46%)	742 (-24%, +46%)	753 (-23%, +51%)	750 (-23%, +53%)
Total [a]	512 (-25%, +55%)	575 (-24%, +56%)	586 (-23%, +61%)	583 (-24%, +65%)
Coal	296 (-48%, +70%)	330 (-49%, +66%)	341 (-49%, +69%)	364 (-48%, +76%)

[a] Emissions from ASGM excluded.

Table 5 The parameters contributing most to emission uncertainties by sector for 2010. The percentages in the parentheses indicate the contributions of the parameters to the variance of corresponding emission estimates.

	CPP	IND	RES
Hg	$\eta_{ESP+FGD}$ (26%)	E_{ASGM} (41%)	EF_{straw} (26%)
	$HgC_{Shandong}$ (21%)	$EF_{NMS\_Zn,\ EP}$ (17%)	AL_{coal} (14%)
Hg^0	$HgC_{Shandong}$ (18%)	E_{ASGM} (39%)	EF_{straw} (41%)
	HgC_{Henan} (8%)	$f_{GM,\ Hg2+}$ (19%)	AL_{straw} (12%)
Hg^{2+}	$HgC_{Shandong}$ (20%)	$f_{GM,\ Hg2+}$ (28%)	HgC_{waste} (28%)
	$f_{ESP+FGD,\ Hg2+}$ (13%)	$EF_{NMS\_Zn,\ EP}$ (22%)	$f_{NOC,\ Hg2+}$ (8%)
Hg^p	$f_{ESP+FGD,\ Hgp}$ (30%)	$f_{WET,\ Hgp}$ (74%)	AL_{coal} (22%)
	$f_{FF,\ Hgp}$ (14%)	$HgC_{Shandong}$ (4%)	$f_{NOC,\ Hg0}$ (15%)

Table 6 Projected national Hg emissions by source category for different scenarios through 2030.

Source category	2015			2020			2030		
	S0	S1	S2	S0	S1	S2	S0	S1	S2
Coal-fired power plants	**150.0**	**149.6**	**130.8**	**164.2**	**153.1**	**130.9**	**181.8**	**155.0**	**126.8**
Industry	**578.1**	**571.1**	**405.4**	**588.0**	**580.9**	**401.4**	**570.9**	**547.6**	**342.5**
Cement production	36.8	36.6	25.4	37.5	37.3	17.2	25.0	24.3	8.9
Coal use	21.1	21.0	13.2	21.7	21.6	11.3	17.6	17.3	8.7
Iron & steel plants	40.0	39.9	39.3	41.7	41.4	39.0	39.8	39.1	34.8
Heating boilers	39.2	37.8	34.2	38.8	37.4	33.8	40.8	36.1	32.3
Other industrial boilers	105.2	101.3	86.4	104.1	100.4	85.4	109.4	96.8	81.7
Nonferrous metal smelting	110.5	109.6	102.4	116.0	115.0	105.5	109.6	106.8	68.2
Zinc	84.5	83.8	78.9	88.7	88.0	81.8	83.8	81.7	56.0
Lead	24.7	24.5	22.3	25.9	25.7	22.4	24.5	23.9	11.0
Copper	1.3	1.3	1.2	1.4	1.3	1.3	1.3	1.3	1.2
Gold mining	182.5	182.4	63.3	183.3	183.1	63.7	182.4	182.0	63.2
Large scale	15.5	15.4	7.7	16.3	16.1	8.1	15.4	15.0	7.5
Artisanal and small scale	167.0	167.0	55.7	167.0	167.0	55.7	167.0	167.0	55.7
Other miscellaneous processes	64.0	63.5	54.3	66.6	66.1	56.7	63.9	62.6	53.4
Mercury mining	34.1	33.8	33.8	35.8	35.5	35.5	33.8	33.0	33.0
Battery/fluorescent lamp production	10.0	10.0	3.3	10.0	10.0	3.3	10.0	10.0	3.3
PVC production	16.8	16.7	14.1	17.7	17.5	14.8	16.7	16.3	13.7
Oil and gas combustion	3.0	3.0	3.0	3.2	3.1	3.1	3.3	3.3	3.3
Residential & commercial sector	**86.0**	**84.2**	**84.2**	**92.0**	**88.4**	**88.4**	**116.7**	**109.9**	**109.9**
Coal burning	37.9	37.0	37.0	37.3	36.4	36.4	34.6	31.6	31.5
Biofuel use/biomass open burning	8.7	8.7	8.7	8.1	8.1	8.1	6.6	6.6	6.6
Solid waste incineration	20.7	20.7	20.7	24.6	24.6	24.6	49.7	49.7	49.7
Municipal	13.9	13.9	13.9	18.5	18.5	18.5	45.1	45.1	45.1
Rural	6.8	6.8	6.8	6.1	6.1	6.1	4.6	4.6	4.6
Oil and gas combustion	18.7	17.8	17.8	22.0	19.3	19.3	25.8	22.0	22.0
Total	**814.1**	**805.0**	**620.4**	**844.3**	**822.5**	**620.7**	**869.3**	**812.5**	**579.1**
Total coal combustion	**393.3**	**386.7**	**340.9**	**407.9**	**390.4**	**336.9**	**423.9**	**375.9**	**315.8**

Figure 1

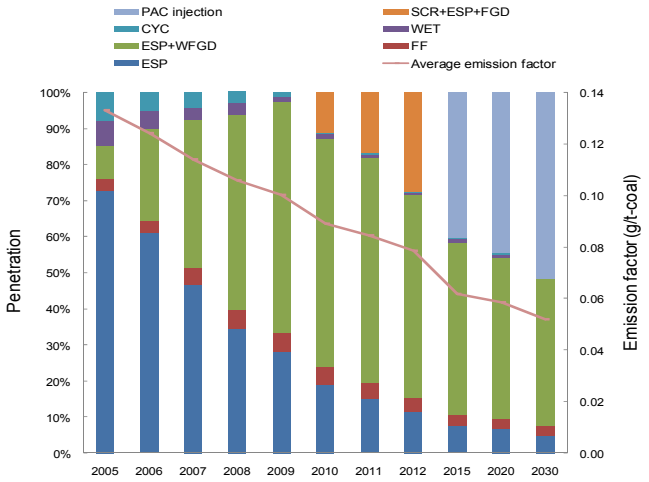

(a) Coal-fired power plants

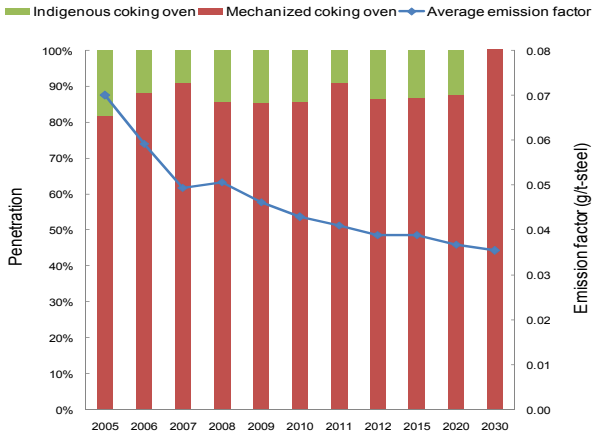

(b) Iron & steel production

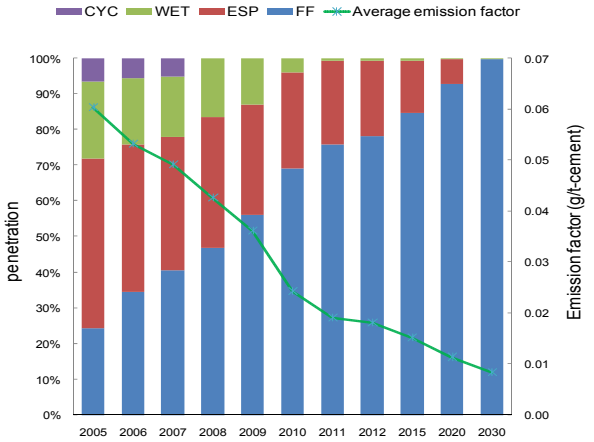

(c) Cement production

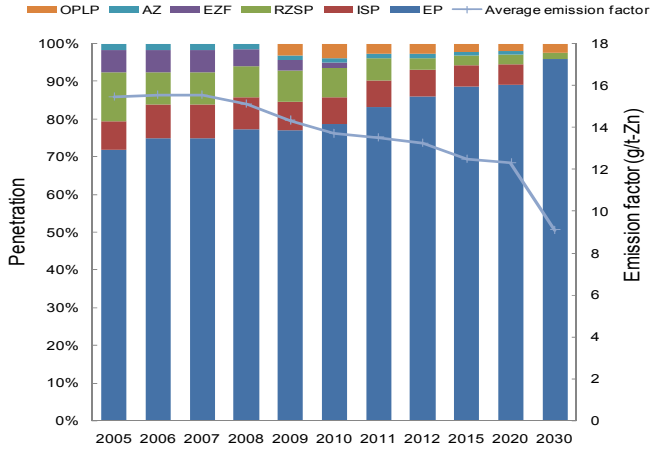

(d) Zn smelting

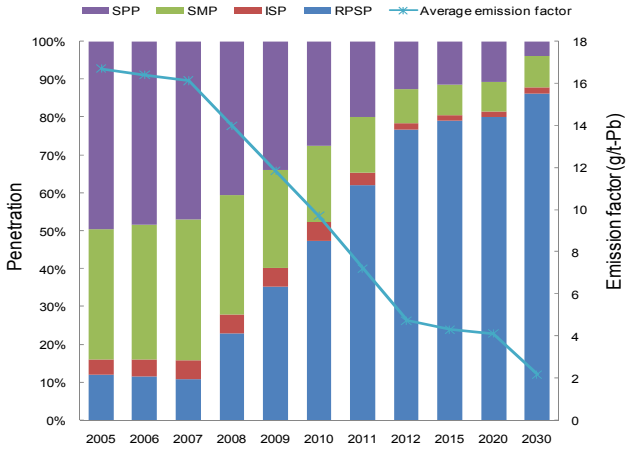

(e) Pb smelting

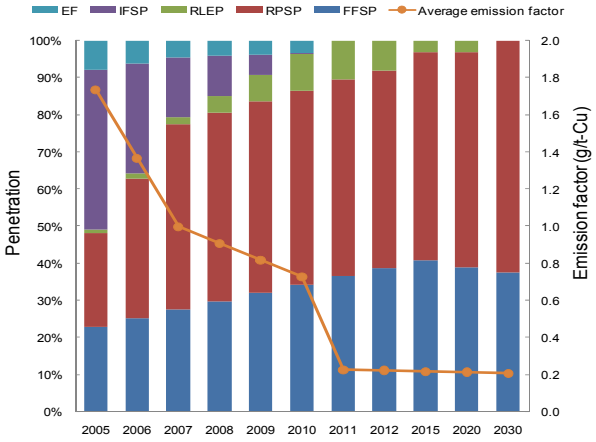

(f) Cu smelting

Figure 2

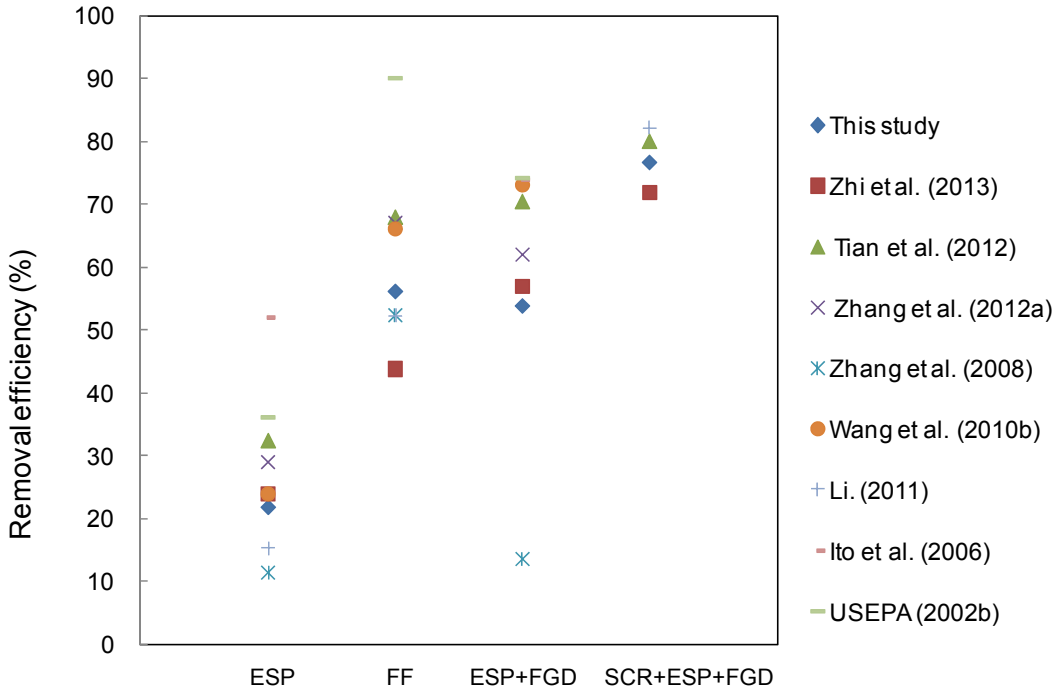
100
90
80
70
60
50
40
30
20
10
0
Removal efficiency (%)
ESP
FF
ESP+FGD
SCR+ESP+FGD
This study
Zhi et al. (2013)
Tian et al. (2012)
Zhang et al. (2012a)
Zhang et al. (2008)
Wang et al. (2010b)
Li. (2011)
Ito et al. (2006)
USEPA (2002b)

Figure 3

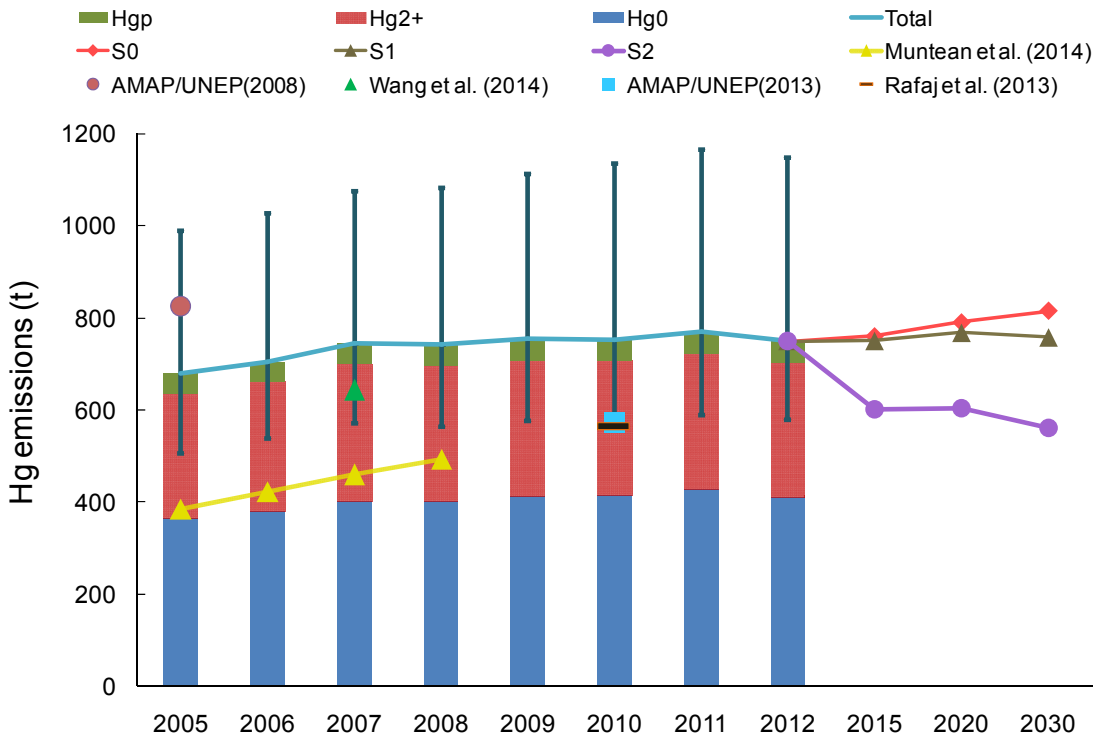
Hgp
Hg2+
Hg0
Total
S0
S1
S2
Muntean et al. (2014)
AMAP/UNEP(2008)
Wang et al. (2014)
AMAP/UNEP(2013)
Rafaj et al. (2013)
Hg emissions (t)
1200
1000
800
600
400
200
0
2005
2006
2007
2008
2009
2010
2011
2012
2015
2020
2030

Figure 4

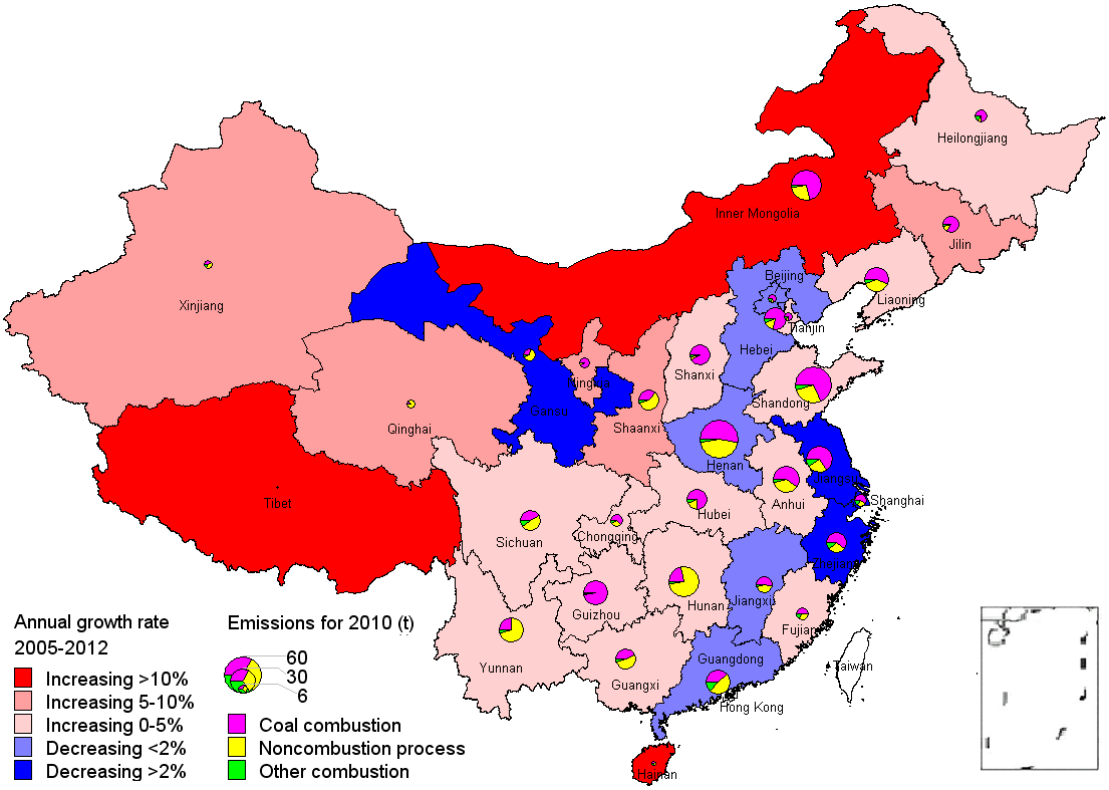
Heilongjiang
Inner Mongolia
Jilin
Xinjiang
Beijing
Liaoning
Tianjin
Hebei
Shanxi
Ningxia
Shandong
Gansu
Shaanxi
Qinghai
Henan
Jiangsu
Shanghai
Tibet
Anhui
Hubei
Sichuan
Chongqing
Zhejiang
Hunan
Jiangxi
Guizhou
Fujian
Guangdong
Yunnan
Guangxi
Taiwan
Hong Kong
Hainan
Annual growth rate
2005-2012
Increasing >10%
Increasing 5-10%
Increasing 0-5%
Decreasing <2%
Decreasing >2%
Emissions for 2010 (t)
60
30
6
Coal combustion
Noncombustion process
Other combustion

Figure 5

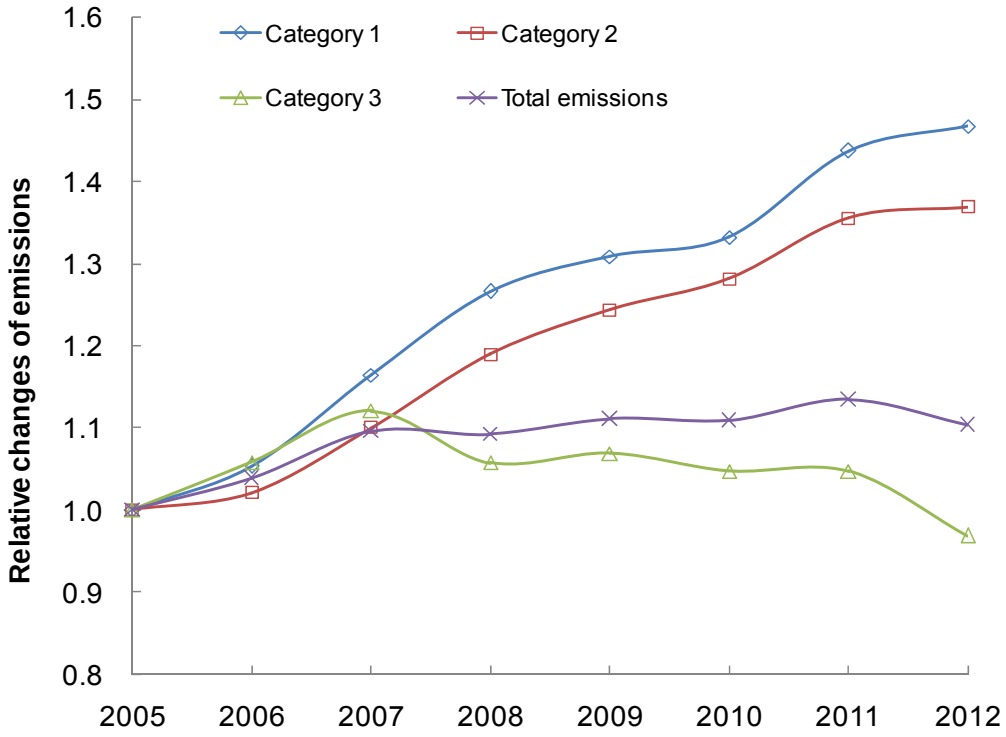
Category 1
Category 2
Category 3
Total emissions
Relative changes of emissions
1.6
1.5
1.4
1.3
1.2
1.1
1.0
0.9
0.8
2005
2006
2007
2008
2009
2010
2011
2012

(a)

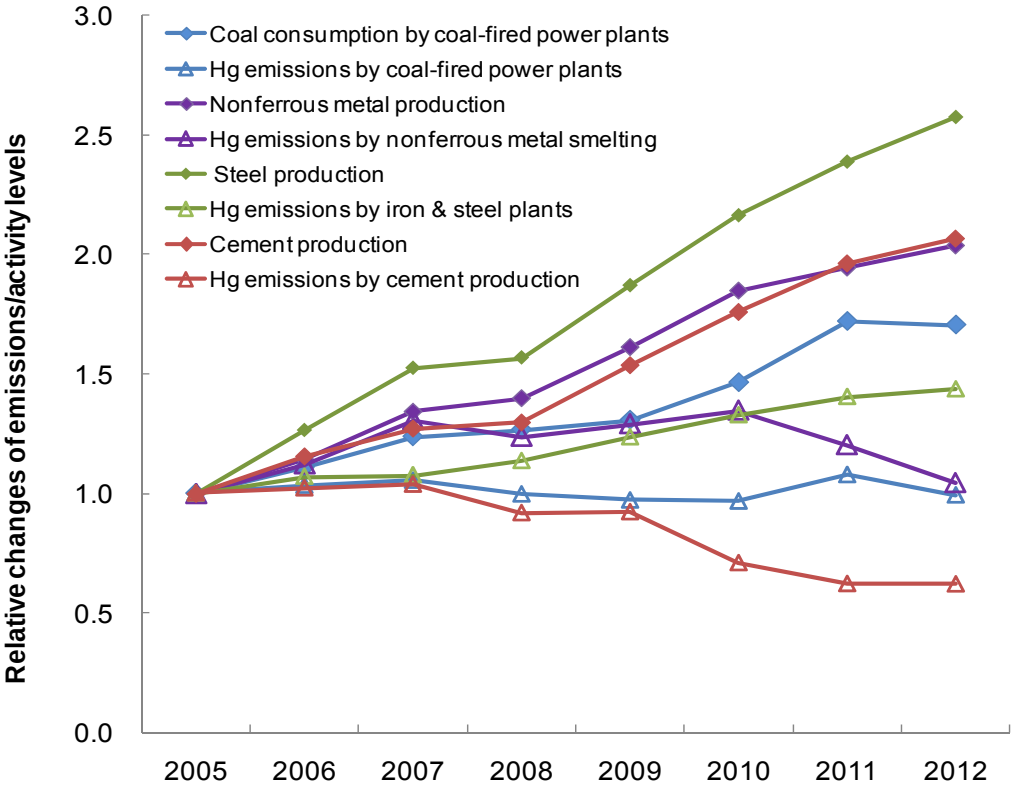
Coal consumption by coal-fired power plants
Hg emissions by coal-fired power plants
Nonferrous metal production
Hg emissions by nonferrous metal smelting
Steel production
Hg emissions by iron & steel plants
Cement production
Hg emissions by cement production
Relative changes of emissions/activity levels
3.0
2.5
2.0
1.5
1.0
0.5
0.0
2005
2006
2007
2008
2009
2010
2011
2012

(b)

Figure 6

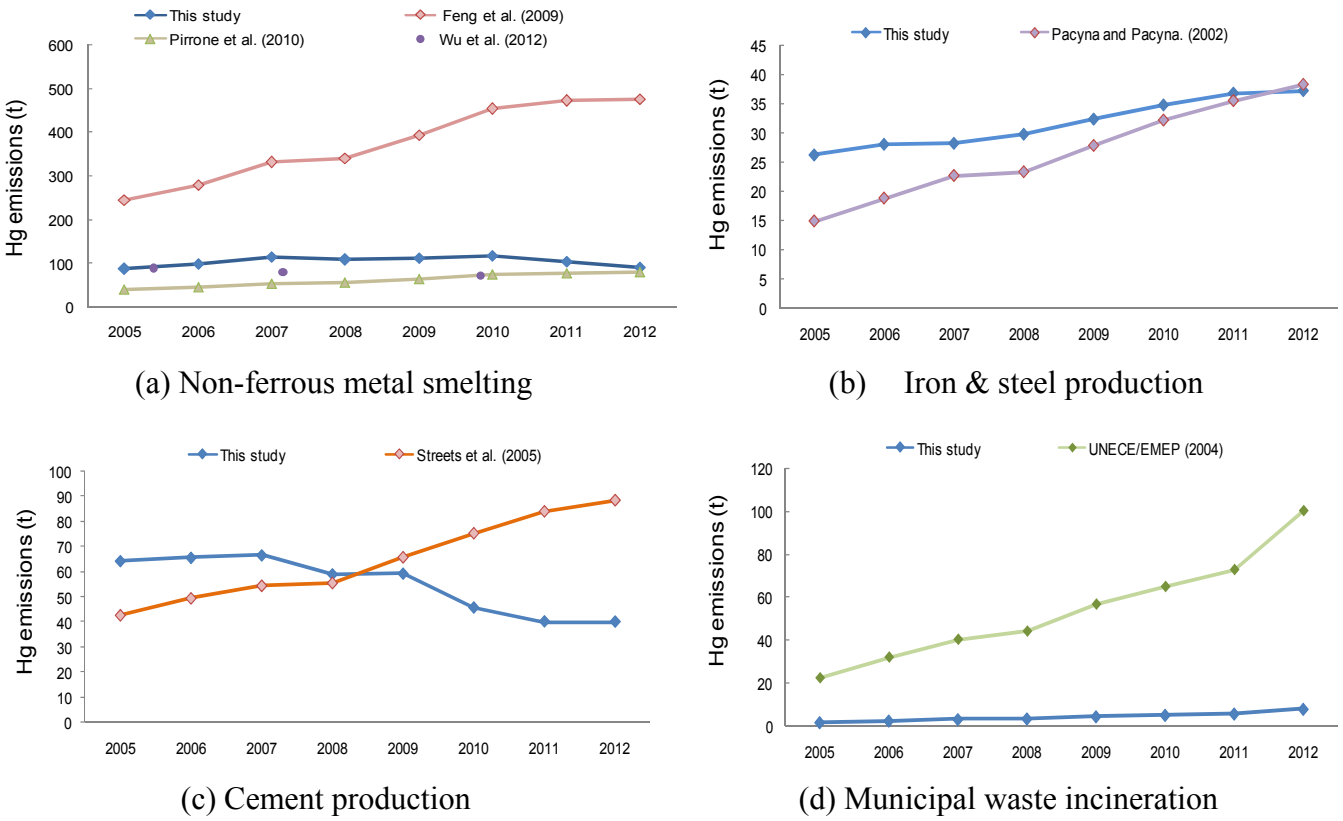

(a) Non-ferrous metal smelting

(b) Iron & steel production

(c) Cement production

(d) Municipal waste incineration

Notes: all the estimates of cited studies except Wu et al. (2012) are not directly obtained from the literatures, but calculated based on the same emission factors suggested by those studies.

Figure 7

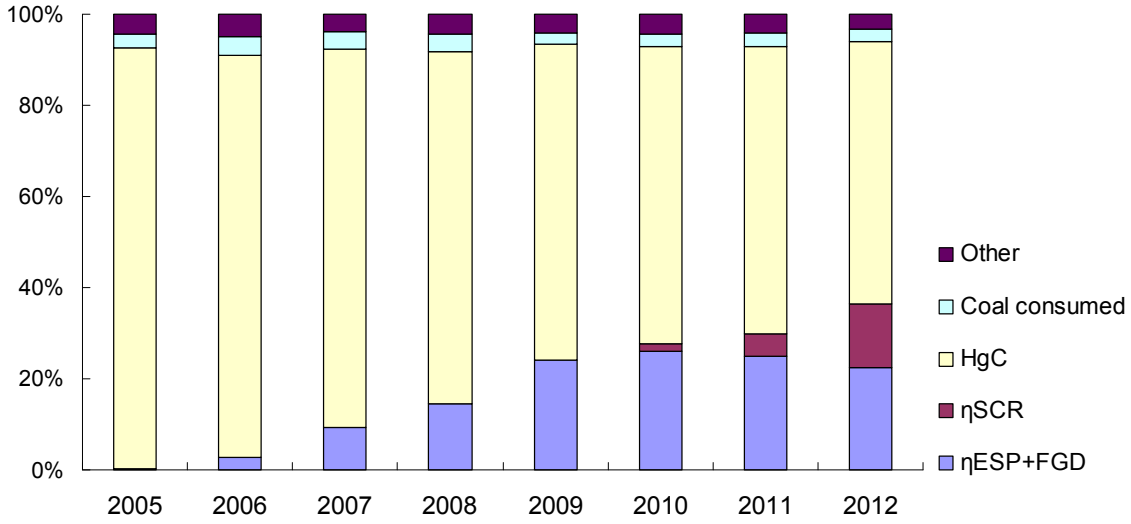
100%
80%
60%
40%
20%
0%
2005
2006
2007
2008
2009
2010
2011
2012
Other
Coal consumed
HgC
ηSCR
ηESP+FGD